数理解析研究所講究録
921 巻 1995 年 58-88

Two-dimensional linear neutral stability of the stationary Burgers vortex layer

Kamen N. Beronov and Shigeo Kida

Research Institute for Mathematical Sciences
Kyoto University, 606–01 Kyoto, Japan

Abstract

A linear stability analysis is presented for a stationary Burgers vortex layer in irrotational straining flow, to normal mode disturbances invariant in the direction of main flow vorticity. The whole neutral curve is calculated by combining numerical and asymptotic analysis. It is similar to that for free mixing layers which are always unstable, except that there is unconditional stability below a critical Reynolds number, in agreement with the long-wave asymptotic result by Neu (*J. Fluid Mech.* **143** (1984) 253). The Reynolds number compares shear flow vorticity versus stretching rate and diffusion, so both latter factors are stabilizing if strong enough. Neutral disturbances represent standing waves.

I. Introduction

Since their discovery by Burgers in 1948, the vortex tube and layer solutions to the Navier-Stokes equations have been regarded as simple models for the local behavior of turbulent flows, and have been accordingly used as the ingredients in vortex-based physical models of fine scales in incompressible turbulence far from boundaries. Experiments and numerical simulations of turbulence show the presence of spatially localized intense vorticity structures. For example, a classification of structures observed in flow simulations (see Ref. 1 and the references therin) shows that the regions of high vorticity fall in two groups, tubes and layers, with relatively low and with comparable strain rate, respectively. Structures with complicated geometry like hair-pin vortices (e.g. in boundary layers), spiral vortices (in mixing layer instabilities), and others seem not to be universal for different flow types and regimes. In contrast, tubes and layers, having the simplest geometry, seem the most general and structurally stable configurations.

The Burgers vortex layer has drawn less attention than the Burgers vortex tube, due to a perception of universality of the Kelvin-Helmholtz instability in turbulent flows and a much more frequent presence of worm-like structures in flow visualizations[2–5], as well as the development of turbulence models based only on cylindrically localized structures. However, layers also appear frequently in simulations[2,3], and reappear in the context of the secondary instabilities of mixing layers[3], e.g. in the regions between "ribs". In the vortex layer evolution, the presence of Kelvin-Helmholtz "rollers" and the subsequent emergence of ribs in the place

of the braids between the rollers are the accepted scenario which has motivated the model of Corcos and Lin[6,7].

The calculations of Lin and Corcos[7] and Neu[8] have pointed out a mechanism of disintegration of viscous vortex sheets into periodic arrays of vortex tubes, given appropriate disturbances and strength of vorticity and external strain. The Burgers vortex tube has been shown to be linearly stable, at least to two-dimensional disturbances[9]. The Kelvin-Helmholtz instability suggests that the Burgers vortex layer is unstable for large Reynolds numbers. A mixing layer not subject to an outer strain field is known to be linearly unstable for *all* Reynolds numbers as implied by the small-wavenumber asymptotic results of Tatsumi and Gotoh[10] and the numerical results of Betchov and Szewczyk[11] (see also Ref. 12, p.157).

There is no profile, however, giving a stationary mixing layer as an exact solution to the Navier-Stokes equations, while the Burgers vortex layer is such a solution when external strain is added. Linear stability has been found for the stagnation-point flows with unidirectional stretching along a plate[13] and at the saddle-point of a curved cylinder[14]. Comparison of known stability results points to the role of orientation of the external irrotational flow, which stabilizes the vortex configuration when it is stretching the vorticity. Thus, the Burgers vortex layer may still be linearly stable, although only for low Reynolds numbers. Indeed, in his analysis of the evolution of integral shear accross a stretched viscous vortex layer, which covers also nonlinear disturbances, but applies only in the small-wavenumber limit, Neu[8] has shown that the linear stability in this limit is restricted to Reynolds numbers below a critical value of order 1. An elaboration[15] of Neu's approach incorporating the first and second momenta of vorticity accross the layer, has confirmed this result and amended the prediction for the growth rate of the disturbances by predicting a short-wave cutoff and verifying the growth-rate estimates given in Ref. 7. The results[8,15] actually imply a positive slope of the neutral curve for linear disturbances, which suggests that the finite threshold found there is indeed the critical Reynolds number. Our purpose in this paper is to show, within the frame of linear stability to two-dimensional disturbances, that this threshold values is indeed the critical Reynolds number, and that there is indeed a short-wave cutoff. The result will be free from assumptions about the particular shape of the disturbances and about smallness of their wavenumbers.

The neutral stability problem is posed and the basic equations are given in Sec. II. Repeating the formulation of the linear stability problem in Lin and Corcos[7], a classical parallel flow linear analysis procedure is followed, leading to an Orr-Sommerfeld type of eigenvalue problem. This is then treated in a different way. Asymptotic analysis is used in Sec. III to study the limiting cases at both ends of the neutral curve. A shooting method is used, as explained in Sec. IV, to find the neutral curve for a range of moderate Reynolds numbers, which is presented together with a simple approximation derived from asymptotic analysis, and the neutral eigenfunctions behavior is shortly discussed. The results are summarized and an outlook on stability problems for stretched viscous vortex structures is given in the concluding remarks. Mathematical derivations needed for the analysis and results detatched from our main topic are presented in four appendices.

II. Formulation

Consider an incompressible viscous flow with constant viscosity ν that is the superposition of a plain stagnation-point flow, which is irrotational and causes hyperbolic stretching, and a viscous vortex layer situated so that its vorticity is stretched by the irrotational component. A time-independent flow of this kind has the form $\boldsymbol{U}(x,y,z) = (U(y), -Ay, Az)$ where A is the strength of the stagnation-point flow. The profile $U(y)$ is uniform in the x- and z-directions, and converges fast to its asymptotic values at infinity. It induces a vorticity field $\boldsymbol{\Omega}(y) = (0, 0, \Omega(y))$ with $\Omega = -U'$ and $\nu\Omega'' + A(y\Omega)' = 0$. Here and further the notations $Df(y) = f'(y) = \mathrm{d}f(y)/\mathrm{d}y$ are used for functions that depend solely on y. Figure 1 gives an illustration of the velocity and vorticity field components. The balance between diffusion and enhancement of vorticity corresponds to a solution of the above ODE[16]. It is frequently called the Burgers vortex layer, and is the flat analog of the better known Burgers vortex tube[17],

$$\Omega(y) = \frac{\Gamma}{\sqrt{2\pi}}\sqrt{\frac{A}{\nu}}\,\exp\left(-\frac{y^2 A}{2\nu}\right). \tag{2.1}$$

The vortex layer strength $\Gamma = U(+\infty) - U(-\infty)$ is so far free to be chosen. We consider the linear stability of this equlibrium solution.

A. Basic equations

The form (2.1) of the equilibrium flow suggests the vortex layer thickness $\delta = \sqrt{\nu/A}$ as the natural unit of length. The convention of taking the asymptotic values for the velocity in shear layers as $U(+\infty) = -U(-\infty)$ fixes the velocity scale $U(+\infty) = \Gamma/2$. The Reynolds number is

$$R = \frac{\Gamma/2}{\sqrt{A\nu}}. \tag{2.2}$$

Note that in Ref. 8 the definition is $R' = \Gamma\delta'/\nu$ and $\delta' = \delta\sqrt{\pi/2}$, so the result for the critical Reynolds number $R'_{cr} = \sqrt{2\pi}$ obtained there corresponds to $R_{cr} = 1$ here. The equations for a disturbance of an equilibrium profile follow from the Navier-Stokes equations:

$$\nabla\cdot\boldsymbol{u} = 0, \tag{2.3}$$

$$\begin{aligned}
\frac{\mathrm{D}u}{\mathrm{D}t} + v\,U'(y) &= -\frac{\partial p}{\partial x} + \frac{1}{R}\nabla^2 u,\\
\frac{\mathrm{D}v}{\mathrm{D}t} - v &= -\frac{\partial p}{\partial y} + \frac{1}{R}\nabla^2 v,\\
\frac{\mathrm{D}w}{\mathrm{D}t} + w &= -\frac{\partial p}{\partial z} + \frac{1}{R}\nabla^2 w,
\end{aligned} \tag{2.4}$$

$$\frac{\mathrm{D}}{\mathrm{D}t} = \frac{\partial}{\partial t} + (\boldsymbol{u}\cdot\nabla) + U(y)\frac{\partial}{\partial x} - y\frac{\partial}{\partial y} + z\frac{\partial}{\partial z}, \tag{2.5}$$

where $\boldsymbol{u}(x,y,z,t) = (u,v,w)$ and $p(x,y,z,t)$ denote the velocity and pressure disturbances. The terms on the left-hand sides in (2.4) produce together the Lagrangian derivatives. The linearized equations for small disturbances follow when $\boldsymbol{u}\cdot\nabla = 0$ in (2.5).

Considering disturbances in unbounded flows, the focus is on their typically better localized vorticity field, rather than on their velocity. The analysis for parallel flows is usually based on the Orr-Sommerfeld equation, which follows from the vorticity disturbance equation. Since the rotational part of the basic flow considered here is only due to a parallel component, the same approach is relevant, considering only two-dimensional, spacially decaying disturbances. These are given by a flow in one of the coordinate planes, which is invariant in the third coordinate, and only the vorticity component along that third coordinate does not vanish. The parallel flow component of the basic flow is y-dependent, which allows for no two-dimensional disturbance in the (x,z)-plane. Compression by main flow strain along the y-direction would inhibit a vorticity component in that direction anyway. A localized two-dimensional disturbance in the (y,z)-plane would decay due to viscous dissipation. The only relevant case is when the vorticity is alligned so as to be stretched by the mean flow strain.

B. Stability problem for normal modes

As in deriving the usual Orr-Sommerfeld equation, one may formally Fourier-transform in the streamwise x-direction and Laplace-transform in time the equations for the disturbane vorticity which follow upon taking the curl of (2.4). The mean flow is not homogeneous in the z-direction, however, and Squire's theorem does not apply. Confining stability analysis only to two-dimensional modes means to accept a nontrivial simplification; three-dimensional linear stability is then left an open problem. The two-dimensional problem reduces to a scalar problem for the linear disturbance streamfunction $\widehat{\phi}(x,y,t)$ with homogeneous boundary conditions. In free flows one has to specify the decay of $u(x,y,t)$ and $v(x,y,t)$, i.e. instead of setting the streamfunction and its normal derivative to zero at a boundary, one specifies the spacial decay rates of $\widehat{\phi}(x,y,t)$ and its gradient. One requires, in the first place, that the Fourier transform in the x-direction could be carried out. Further, we are interested in well localized disturbances, which decay fast outside the shear layer, so that the stabillity result for the Burgers vortex layer model carries over to localized events in more complicated flows. The normal modes are the Fourier-Laplace components, which now depend on the non-dimensional phase speed $c(\alpha,R)=c_r+ic_i$ and the real wavenumber α. For an individual normal mode

$$\widehat{\phi}(x,y,t)=\phi(y)\,e^{i\alpha(x-ct)},\qquad u(x,y,t)=\frac{\mathrm{d}\phi}{\mathrm{d}y}\,e^{i\alpha(x-ct)},\qquad v(x,y,t)=i\alpha\,\phi(y)\,e^{i\alpha(x-ct)}. \tag{2.6}$$

The exponential growth rate of the mode is $\alpha\,c_i$. These modes arise[12] from the decomposition of eigenfunctions of Orr-Sommerfeld type eigenvalue problems. The possible contribution from a continuous spectrum is not considered here. From the vorticity equation for a normal mode disturbance one obtains the ODE

$$(D^2+yD+1-\alpha^2)(\phi''-\alpha^2\phi)-i\alpha R\,((U(y)-c)(\phi''-\alpha^2\phi)-U''(y)\phi)=0, \tag{2.7}$$

henceforth called the Orr-Sommerfeld equation. Together with decay conditions for the eigenfunction $\phi(y)$, it defines a generalized eigenvalue problem for $c(\alpha,R)$, that is, a problem of the type $A\,\phi=c\,B\,\phi$ where A and B are linear operators which may be integral or differential and generally be not invertible.

The ordinary differential operator originating from the Laplacian in the underlying Navier-Stokes equations will henseforth be called the "Laplacian" as well, although it is sometimes named "modified Laplacian" in the literature, and is formally a Helmholtz operator for imaginary frequency $k=i\alpha$:

$$\nabla_\alpha^2 = D^2 - \alpha^2 . \tag{2.8}$$

An equivalent form of (2.7) is the system

$$(\nabla_\alpha^2 + D\,y)\omega = i\,\alpha R((U-c)\omega - U''\phi), \qquad \nabla_\alpha^2\phi = \omega , \tag{2.9}$$

where $-\omega(y)$ is the disturbance vorticity. Without causing confusion, the function $\omega(y)$ will henceforth be called the "vorticity" and $\phi(y)$ the "streamfunction".

What will be meant by a well localized disturbance is one with a sufficiently fast spacial decay at infinity of *vorticity*. Hereafter it will be assumed to decay at least exponentially,

$$\exists\ \sigma, A_\omega > 0,\ \ p_\omega \geq 0\ :\qquad |\omega(y)| < A_\omega |y|^{p_\omega} \exp(-\sigma|y|) . \tag{2.10}$$

The linear operator ∇_α^2 has an exponentially decaying Green function (see Appendix C) and an inverse ∇_α^{-2} which is bounded in the L_2 and the L_∞, and which leaves the space of functions satisfying (2.10) with $\sigma=\alpha$ invariant. It defines $\phi(y)$ uniquely from $\omega(y)$, so a closed equation for $\omega(y)$ follows from (2.9), giving a standard eigenvalue problem in terms of $\omega(y)$ and c. It will further follow from the asymptotic analysis and Appendix B, that $\nabla_\alpha^2 + D\,y$ is invertible on functions satisfying (2.10) for some $\sigma > 0$, when $0 < \alpha < 1$, and that $I - (U''/U)\nabla_\alpha^{-2}$ is invertible for $0 < \alpha < 0.733$.

III. Asymptotic analysis

The definition of ∇_α^{-2}, as well as the forms of the eigenvalue and the differential equation depend on α and R analytically through the parameters α^2 and αR. Whenever any of the latter becomes small or large, it is appropriate to study the asymptotic limit for the solution.

A. Small-wavenumber asymptotics

In this limit it is assumed that

$$R = \mathrm{O}(1) \qquad \text{and} \qquad \alpha \ll 1 . \tag{3.1}$$

The eigenfunctions are expanded as

$$\omega(y) = \omega_0(y) + \alpha\,\omega_1(y) + \alpha^2\omega_2(y) + \cdots , \tag{3.2}$$

while an expansion of ∇_α^{-2} suggests (cf. Appendix C) that

$$\phi(y) = \frac{1}{\alpha}\,\phi_0(y) + \phi_1(y) + \alpha\,\phi_2(y) + \cdots . \tag{3.3}$$

To find an asymptotic approximation to the neutral curve it is further necessary to expand the Reynolds number, and the curve is conveniently parametrized by the wavenumber, as suggested by the numerical results (see Fig. 2(b) below):

$$R(\alpha) = R_0 + \alpha R_1 + \alpha^2 R_2 + \cdots, \qquad \mathcal{I}m\, R_n = 0, \quad n = 0, 1, 2, \ldots, \qquad R_0 \geq 0. \tag{3.4}$$

Using the definitions

$$\lambda = \alpha^2 - i\alpha c R, \qquad \mathcal{M} = D(D+y), \tag{3.5}$$

eqs. (2.9), can be put as a standard eigenvalue problem, $(\mathcal{M} - i\alpha R\,(U(y) - U''(y)\,\nabla_\alpha^{-2}))\,\omega = \lambda\omega$. From the definition of λ one has $c = \frac{i}{R}\left(\frac{\lambda}{\alpha} - \alpha\right)$ and $c_i = 0 \Leftrightarrow \lambda_r = \alpha^2$. Along the neutral curve the eigenvalue is expanded as

$$\lambda(\alpha) = \lambda_0 + \alpha\lambda_1 + \alpha^2\lambda_2 + \cdots, \qquad \lambda_{r\,n} = 0 \text{ for } n \neq 2, \qquad \lambda_{r\,2} = 1. \tag{3.6}$$

a. Expansion equations

Using the expansions (3.2)–(3.6) to substitute for $\omega(y)$, $\phi(y)$, R, λ, one finds upon equating terms at equal powers of α the equations for the successive approximations:

$$\mathcal{M}\omega_0 = \lambda_0\omega_0 - iR_0U''(y)\phi_0, \tag{3.7}$$

$$\mathcal{M}\omega_n = \sum_{j=0}^{n}\lambda_j\omega_{n-j} + i\sum_{j=0}^{n-1} R_j(U(y)\omega_{n-j-1} - U''\phi_{n-j}) - iR_nU''(y)\phi_0, \qquad n \geq 1. \tag{3.8}$$

The equation $\nabla_\alpha^2\phi = \omega$ can be explicitly solved, using (C.5) and (C.6) from Appendix C, $\phi(y) = \nabla_\alpha^{-2}\omega$ and leading terms in α of $\phi(y)$ depend only on corresponding leading terms of $\omega(y)$. Using this and the Hermite functions defined by (B.1) and (B.8) in Appendix B, one obtains

$$\mathcal{M}\omega_0 = \lambda_0\omega_0(y) + iR_0\left(\frac{h_1(y)}{2}\int_{-\infty}^{+\infty}\omega_0(y_1)\,dy_1\right), \tag{3.9}$$

$$\begin{aligned}\mathcal{M}\omega_1 = {} & \lambda_0\omega_1 + \lambda_1\omega_0 \\ & + iR_0\left(h_{-1}(y)\omega_0 + \frac{h_1(y)}{2}\left(\int_{-\infty}^{+\infty}\omega_1(y_1)\,dy_1 - \int_{-\infty}^{+\infty}|y-y_1|\,\omega_0(y_1)\,dy_1\right)\right) \\ & + iR_1\left(\frac{h_1(y)}{2}\int_{-\infty}^{+\infty}\omega_0(y_1)\,dy_1\right),\end{aligned} \tag{3.10}$$

$$\begin{aligned}\mathcal{M}\omega_2 = {} & \lambda_0\omega_2 + \lambda_1\omega_1 + \lambda_2\omega_0 \\ & + iR_0\left(h_{-1}(y)\omega_1 + \frac{h_1(y)}{2}\left(\int_{-\infty}^{+\infty}\omega_2(y_1)\,dy_1 - \int_{-\infty}^{+\infty}|y-y_1|\,\omega_1(y_1)\,dy_1\right.\right. \\ & \qquad \left.\left. + \frac{1}{2}\int_{-\infty}^{+\infty}(y-y_1)^2\omega_0(y_1)\,dy_1\right)\right) \\ & + iR_1\left(h_{-1}(y)\omega_0 + \frac{h_1(y)}{2}\left(\int_{-\infty}^{+\infty}\omega_1(y_1)\,dy_1 - \int_{-\infty}^{+\infty}|y-y_1|\,\omega_0(y_1)\,dy_1\right)\right) \\ & + iR_2\left(\frac{h_1(y)}{2}\int_{-\infty}^{+\infty}\omega_0(y_1)\,dy_1\right),\end{aligned} \tag{3.11}$$

$$
\begin{aligned}
\mathcal{M}\omega_3 &= \lambda_0\omega_3 + \lambda_1\omega_2 + \lambda_2\omega_1 + \lambda_3\omega_0 \\
&+ iR_0\left(h_{-1}(y)\omega_2 + \frac{h_1(y)}{2}\left(\int_{-\infty}^{+\infty}\omega_3(y_1)\,dy_1 - \int_{-\infty}^{+\infty}|y-y_1|\omega_2(y_1)\,dy_1\right.\right. \\
&\qquad \left.\left. + \frac{1}{2}\int_{-\infty}^{+\infty}(y-y_1)^2\omega_1(y_1)\,dy_1 - \frac{1}{6}\int_{-\infty}^{+\infty}|y-y_1|^3\omega_0(y_1)\,dy_1\right)\right) \\
&+ iR_1\left(h_{-1}(y)\omega_1 + \frac{h_1(y)}{2}\left(\int_{-\infty}^{+\infty}\omega_2(y_1)\,dy_1 - \int_{-\infty}^{+\infty}|y-y_1|\omega_1(y_1)\,dy_1\right.\right. \\
&\qquad \left.\left. + \frac{1}{2}\int_{-\infty}^{+\infty}(y-y_1)^2\omega_0(y_1)\,dy_1\right)\right) \\
&+ iR_2\left(h_{-1}(y)\omega_0 + \frac{h_1(y)}{2}\left(\int_{-\infty}^{+\infty}\omega_1(y_1)\,dy_1 - \int_{-\infty}^{+\infty}|y-y_1|\omega_0(y_1)\,dy_1\right)\right) \\
&+ iR_3\left(\frac{h_1(y)}{2}\int_{-\infty}^{+\infty}\omega_0(y_1)\,dy_1\right), \qquad (3.12)
\end{aligned}
$$

and so on, where the unknown functions are only $\omega_n(y)$ subject to (2.10).

b. Leading order

Let $h_\lambda(y)$ denote any eigenfunction satisfying (2.10) and $\mathcal{M}h_\lambda = \lambda h_\lambda$. The latter is exactly (B.2) in Appendix B, so one may use the decay rate of the general solutions given by the asymptotics (B.5) to reject all solutions except those for $\lambda_0 = 0, -1, -2, \ldots$. In particular, one has from (B.8) $\mathcal{M}h_0 = 0$, $\mathcal{M}h_1 = -h_1$ Solving separately for both terms in the right-hand side in (3.9), then adding an arbitrary fast decaying solution to the homogeneous equation defined by the left-hand side operator $\mathcal{M}$, and finally integrating and using (B.1) to relate the coefficients at the separate solution components, one obtains the general fast decaying leading-order solution in the form

$$
\begin{aligned}
\omega_0(y) &= \begin{cases} C_1\,(h_0(y) - iR_0\,h_1(y)) & \text{if} \quad n = 0 \\ C_1\,h_n(y) + C_0\,(h_0(y) - iR_0\,h_1(y)) & \text{if} \quad n = 1,2,\ldots \end{cases} \qquad (3.13) \\
C_0, C_1 &= \text{const.}, \qquad C_1 \neq 0\,.
\end{aligned}
$$

The constants must be chosen as a way to normalize the whole eigenfunction $\omega(y)$. When $\lambda_0 = -n$, $n \geq 1$, the growth rate is to leading order $\alpha c_i = -n/R$ for $\alpha \ll 1$. This means very strong damping and is closely reminiscent of the $\alpha R \to 0$ limit behavior for channel flows (see Ref. 12, p.158), where $c_i \sim (\alpha R)^{-1}$, and the critical Reynolds number is positive. For the only mode which is neutrally stable to leading order, one has from (3.13)

$$
\lambda_0 = 0\,, \qquad \omega_0(y) = h_0(y) - iR_0\,h_1(y)\,. \qquad (3.14)
$$

This normalization is consistent with the one used in §IV.3 below for numerically computed eigenfunctions. In (3.13) it was chosen $C_1 = 1$ and (see (B.9) in Appendix B)

$$
\int_{-\infty}^{+\infty}\omega_0(y)\,dy = 2\,, \qquad \phi_0(y) = -1\,. \qquad (3.15)
$$

Because all fast decaying functions in the kernel of $\mathcal{M}$ are spanned by $h_0(y)$, any such component in $\omega_n(y)$, $n \geq 1$, can be absorbed from the start into the leading-order Gaussian component.

c. First order

Inserting (3.14) into (3.10), evaluating the integrals according to (D.5) and (D.6) and using the relations (D.1) between the Hermite functions $h_n(y)$, given in Appendix D, the first-order equation may be put in the form

$$\begin{aligned}\mathcal{M}\omega_1 &= \lambda_1(h_0 - iR_0 h_1) + iR_1 h_1 \\ &\quad + iR_0\left(h_{-1}(h_0 - iR_0 h_1) - h_1\left(h_0 + y\,h_{-1} - iR_0 h_{-1} - \frac{1}{2}\int_{-\infty}^{+\infty}\omega_1(y_1)\,dy_1\right)\right) \\ &= \lambda_1 h_0 + i\,h_1\left(R_1 - R_0\left(\lambda_1 - \frac{1}{2}\int_{-\infty}^{+\infty}\omega_1(y_1)dy_1\right)\right) \\ &\quad + iR_0\frac{d}{dy}(h_{-1}^2 - h_0^2 + h_{-1}h_1)\,. \end{aligned} \tag{3.16}$$

The solvability condition (B.15) immediately gives

$$\lambda_1 = 0\,. \tag{3.17}$$

Making use of (B.8) and (B.14), one obtains

$$\begin{aligned}\omega_1(y) &= -i\left(R_1 + \frac{R_0}{2}\int_{-\infty}^{+\infty}\omega_1(y_1)dy_1\right)h_1(y) \\ &\quad -iR_0\,h_0(y)\int_0^y\left(\frac{1-h_{-1}^2(y_1)}{h_0(y_1)} + h_0(y_1) + y_1\,h_{-1}(y_1)\right)dy_1 \end{aligned} \tag{3.18}$$

with the Gaussian component being absorbed into ω_0 as mentioned above. Noting that all terms in ω_1 are odd and fast decaying, so that $\int_{-\infty}^{+\infty}\omega_1(y_1)\,dy_1 = 0$, and further that $\int_0^y y_1\,h_{-1}(y_1)\,dy_1 = \frac{1}{2}\,(y^2 h_{-1}(y) - \int_0^y y_1^2\,h_0(y_1)\,dy_1) = \frac{1}{2}((y^2-1)h_{-1}(y) - h_1(y))$ which implies $h_0(y)\int_0^y (h_0(y_1) + y_1 h_{-1}(y_1))\,dy_1 = h_0 h_{-1} + \frac{1}{2}(h_2 h_{-1} - h_0 h_1)$, where (D.1) have been used again, one finds

$$\begin{aligned}\omega_1(y) &= -iR_1\,h_1(y) - iR_0\,g_1(y)\,, \\ g_1(y) &= h_0(y)\int_0^y\frac{1-h_{-1}^2(y_1)}{h_0(y_1)}dy_1 + \frac{1}{2}\frac{d}{dy}(h_{-1}^2 - h_0^2 + h_{-1}h_1)\,. \end{aligned} \tag{3.19}$$

d. Second order

As a first step one seeks to simplify the second-order equation (3.11). It was already found that $\lambda_0 = 0$ and that ω_1 is odd and fast decaying (see (3.14) and (3.18)). Using (D.7) and (D.8) from Appendix D, one evaluates $\frac{1}{4}\int_{-\infty}^{+\infty}(y-y_1)^2\omega_0(y_1)\,dy_1 = \frac{1}{2}(y^2+1) - iR_0\,y$. Then using (D.5) and (D.6), $\frac{1}{2}\int_{-\infty}^{+\infty}|y-y_1|\,\omega_0(y_1)\,dy_1 = (y\,h_{-1} + h_0) - iR_0\,h_{-1}$, and applying some of the transformations (D.1), one finds

$$\begin{aligned}\mathcal{M}\omega_2 &= \lambda_2(h_0 - iR_0\,h_1) + iR_2\,h_1 + iR_1\,h_0\,((y^2+1)\,h_{-1} - h_1) \\ &\quad + iR_0\left(h_{-1}\,\omega_1 + h_1\left(\frac{y^2+1}{2} - iR_0\,y\right.\right. \\ &\quad \left.\left. -\frac{1}{2}\int_{-\infty}^{+\infty}|y-y_1|\,\omega_1(y_1)\,dy_1 + \frac{1}{2}\int_{-\infty}^{+\infty}\omega_2(y_1)\,dy_1\right)\right)\,. \end{aligned} \tag{3.20}$$

Applying now the solvability condition (B.15), noting that decaying odd integrands give no contribution in integration over the whole real axis, and using (D.11) to cancel the terms with the integrand ω_1, one obtains $0 = 2(\lambda_2 - R_0^2)$. This and the restrictions in (3.4) and (3.6) imply

$$\lambda_2 = 1, \qquad R_0 = 1. \tag{3.21}$$

To settle the question about the critical Reynolds number of the Burgers vortex layer, it is shown below that $R_1 > 0$ which confirms that $R_{cr} = R_0 = 1$ and is supported by the numerical results for $\alpha = O(1)$ (see Fig. 2(b)). That the neutral curve has its left end at a finite Reynolds number, as given by (3.21) in our case, is a difference both from free shear layers, which are always linearly unstable with $R_{cr} = 0$, and from channel flows, where $R_1 > 0$ but there exists also a lower branch of the neutral curve extending to infinity in R.

e. Third order

Taking into account the results up to second order and transforming terms in the same way as in the derivation of (3.20), equation (3.12) can be put in the somewhat simpler form

$$\begin{aligned}
\mathcal{M}\omega_3 = {} & \lambda_3(h_0(y) - ih_1(y)) + \omega_1(y) \\
& + iR_3 h_1(y) + iR_2 h_0(y)((y^2+1)h_{-1}(y) - h_1(y)) \\
& + iR_1 \left(h_{-1}(y)\omega_1(y) + h_1(y) \left(\frac{1}{2}\int_{-\infty}^{+\infty} \omega_2(y_1)\,dy_1 \right.\right. \\
& \qquad \left.\left. - \frac{1}{2}\int_{-\infty}^{+\infty} |y-y_1|\omega_1(y_1)\,dy_1 + \frac{y^2+1}{2} - iy \right) \right) \\
& + i \left(h_{-1}(y)\omega_2(y) + h_1(y)\frac{1}{2} \left(\int_{-\infty}^{+\infty} \omega_3(y_1)\,dy_1 - \int_{-\infty}^{+\infty} |y-y_1|\omega_2(y_1)\,dy_1 \right.\right. \\
& \qquad \left.\left. + \frac{1}{2}\int_{-\infty}^{+\infty} (y-y_1)^2\omega_1(y_1)\,dy_1 - \frac{1}{6}\int_{-\infty}^{+\infty} |y-y_1|^3\omega_0(y_1)\,dy_1 \right) \right).
\end{aligned} \tag{3.22}$$

Applying the solvability condition, i.e. integrating and recognizing all vanishing integrals, and then using (D.11) to cancel terms which have $|y-y_1|\omega_1(y_1)$ and $|y-y_1|\omega_2(y_1)$ integrands, as it was done for the second-order equation, one finds that

$$0 = 2(\lambda_3 - R_1) + i\int_{-\infty}^{+\infty} dy\, h_1(y) \int_{-\infty}^{+\infty} dy_1 \left(\frac{(y-y_1)^2}{4}\omega_1(y_1) - \frac{|y-y_1|^3}{12}\omega_0(y_1) \right).$$

Applying (D.1) and (D.12), one evaluates the first integral above as

$$\begin{aligned}
i\int_{-\infty}^{+\infty} y\,\omega_1(y)\,dy &= \int_{-\infty}^{+\infty} \left(R_1 y h_1 - h_1 \int_0^y \left(\frac{1-h_{-1}^2}{h_0} + h_0 + y_1 h_{-1} \right) dy_1 \right) dy \\
&= -2R_1 + \int_{-\infty}^{+\infty} \left(1 - h_{-1}^2 + 2h_0^2 \right) dy \;=\; -2R_1 + \frac{8}{\sqrt{\pi}},
\end{aligned}$$

since $\int_{-\infty}^{+\infty}(1-h_{-1}^2)\,dy = 2\int_{-\infty}^{+\infty} y\,h_0 h_{-1}\,dy = 2\int_{-\infty}^{+\infty} h_0^2\,dy = \frac{4}{\sqrt{\pi}}$. For the second integral one recalls the solutions at lower orders, (3.14) and (3.21), then applies (D.13) and uses again (D.1):

$$-\frac{i}{2}\int_{-\infty}^{+\infty} \left((y^2+1)h_{-1} - h_1 \right)(h_0 - ih_1)\,dy = \frac{1}{2}\int_{-\infty}^{+\infty} \left((h_3 + 4h_1)h_{-1} - h_1^2 \right) = 2\int_{-\infty}^{+\infty} h_0^2\,dy. \tag{3.23}$$

The final form of the solvability condition then reads $0=\lambda_3-2R_1+6/\sqrt{\pi}$. Recalling that R_1 is real and λ_3 is pure imaginary, one finds $\lambda_3=0$ and $R_1=3/\sqrt{\pi}=1.6926$, i.e. $R_1>0$ indeed. To this order, $c(\alpha)=O(\alpha^3)$ and

$$\lambda=\alpha^2+O\left(\alpha^4\right), \qquad R=1+\frac{3}{\sqrt{\pi}}\alpha+O\left(\alpha^2\right). \tag{3.24}$$

B. Large-Reynolds-number asymptotics

In this limit it is assumed that

$$\alpha=O(1), \quad R\gg 1 \qquad \text{and} \qquad \epsilon=\frac{1}{\alpha R}\ll 1. \tag{3.25}$$

The parametrization at this end of the neutral curve (see Fig. 2) is conveniently taken as $\alpha_{cr}(\epsilon)$. An eigenvalue problem formulation in terms of the streamfunction will be used. To this end, equation (2.9) is written using (3.25) as

$$U(y)\left(\nabla_\alpha^2+K(y)\right)\phi(y)=\left(c-i\,\epsilon(\nabla_\alpha^2+Dy)\right)\nabla_\alpha^2\,\phi(y), \tag{3.26}$$

$$K(y)=-U''(y)/U(y). \tag{3.27}$$

For general smooth, *odd, monotonous* profiles $K(y)$ is a smooth *even* function, which decays like $U''(y)$ if the asymptotic values of the profile are nonzero at both infinities. $K(y)$ is strictly positive for the profile considered here, as well as for the popular choice $U(y)=\tanh(y)$. On the neutral curve

$$\phi_{cr}(y)=\phi_0(y)+\epsilon\,\phi_1(y)+\epsilon^2\,\phi_2(y)+\cdots, \tag{3.28}$$

$$\alpha_{cr}^2(\epsilon)=a_0+\epsilon\,a_1+\epsilon^2 a_2+\cdots, \tag{3.29}$$

$$c_{cr}(\epsilon)=c_0+\epsilon\,c_1+\epsilon^2 c_2+\cdots, \tag{3.30}$$

$$\mathcal{I}m\;c_n=0, \qquad n=0,1,2,\ldots, \tag{3.31}$$

are assumed to hold. The wavenumber expansion $\alpha_{cr}=\alpha_0+\epsilon^2\alpha_1+\ldots$ is equivalent but less convenient; note that

$$a_0=\alpha_0^2, \qquad \alpha_{cr}(\epsilon)=\sqrt{a_0}+\epsilon\frac{a_1}{2\sqrt{a_0}}+O\left(\epsilon^2\right). \tag{3.32}$$

Substitution of (3.28), (3.30) and (3.31) into (3.26) leads to the simplest perturbation scheme in the nviscid limit, which is not readily extended beyond first order (see Ref. 19, Chapter 8). (The difficulties due to the *singular perturbation* nature of the inviscid limit for the usual Orr-Sommerfeld equation have been considered in great detail in the past[12,19]. In the present case $y=0$ is not a turning point, because of the profile symmetry, and viscous solutions play no role in the large Reynolds number limit.) It is convenient to introduce the "leading-order Laplacian" $\nabla_0^2=D^2-\alpha_0^2$; the Laplacian is expanded as $\nabla_\alpha^2=\nabla_0^2-\epsilon\,a_1-\epsilon^2 a_2-\ldots$. The resulting formal perturbation scheme reads

$$U(y)\left(\nabla_0^2+K(y)\right)\phi_0=c_0\nabla_0^2\,\phi_0, \tag{3.33}$$

$$U(y)\left(\nabla_0^2+K(y)\right)\phi_1=c_0\nabla_0^2\,\phi_1+\left(c_1\nabla_0^2+(U(y)-c_0)\,a_1\right)\phi_0-i(\nabla_0^2-Dy)\,\nabla_0^2\,\phi_0, \tag{3.34}$$

etc. The leading order is given by the Rayleigh equation (3.33) and defines an eigenvalue problem. The equations at higher orders have the general form $U(y)\,(\nabla_0^2+K(y))\,\phi_n = c_0\nabla_0^2\,\phi_n + F_n$ in which the inhomogeneous term F_n depends only on a_n and on the solution to lower orders. In these equations, a solvability condition has to be satisfied, which effectively defines the correction terms in the expansions of c_{cr} and α_{cr}^2, similarly to the way the corrections to λ and R were determined in the small-wavenumber expansion. The boundary condition is given again by the fast decay requirement (2.10), and the eigenfunction is normalized in the same way as in the small-wavenumber expansion. This is justified *a posteriori* in the inviscid neutral case, where it turns out that the eigenfunction does not vanish at the origin.

a. Leading order

For the Rayleigh equation rigorous qualitative results have been established by Howard[18], which imply that there exists at most one unstable or neutrally stable mode $\phi_0(y)$ and $c_r(\alpha)=0$ for odd, monotonous profiles with $U''(0)=U(0)=0$ and $U''(y)\neq 0$ for $y\neq 0$. For the neutral disturbance $c_i(\alpha)=0$ holds as well, so the real and imaginary parts separate, and (3.33) becomes a *real* eigenvalue problem for α_0 and $\phi_0(y)$. From the profile symmetry it is clear that the eigenfunction is either even or odd. The results in Ref. 18 are based on a comparison of the Rayleigh problem to a Sturm-Liouville problem, which actually coincide in the neutral case. The leading (fundamental) mode of a Sturm-Liouville problem has no zero crossings, so $\phi_0(y)$ and hence $\omega(y)$ must be even. They satisfy $\omega(y)=-K(y)\,\phi(y)$ and $\phi''(y)=(\alpha^2-K(y))\,\phi(y)$ where α is the eigenvalue. Here $K^{(2n+1)}(0)=0$, $K(0)=1$, $K''(0)=-\frac{2}{3}$, $K^{(4)}(0)=\frac{16}{15}$, etc. One may identify successively all derivatives $\omega^{(2n)}(0)$ and $\phi^{(2n)}(0)$ as polynomials in α^2, proving that the eigenfunctions are analytic in α. In particular, $\omega(0)=-\phi(0)=1$, $\phi''(0)=1-\alpha^2$, $\omega''(0)=\alpha^2=-5/3$. The numerical result includes the normalized eigenfunction shown in Fig. 4 and the eigenvalue. One has

$$\int_{-\infty}^{+\infty}\phi_0^2(y)\,dy = 2.832\,, \qquad a_0 = 0.537\,, \qquad \alpha_{cr}=\sqrt{a_0}=0.733\,. \tag{3.35}$$

b. First order

The solvability condition can be found by noting that ϕ_0 is fast decaying and ∇_0^2 is self-adjoint. Applying $\int_{-\infty}^{+\infty}dy\,\phi_0(y)/U(y)$ to both sides of (3.34) and using $c_0=0$ and $\nabla_0^2\,\phi_0=-K\phi_0$, one finds

$$0 = a_1\int_{-\infty}^{+\infty}\phi_0^2(y)\,dy \;-\; \int_{-\infty}^{+\infty}\frac{\phi_0(y)}{U(y)}\left(c_1 - i\,(\nabla_0^2+Dy)\right)K\,\phi_0\,dy\,. \tag{3.36}$$

In the second integral all integrands are odd because ϕ_0 is even and $U(y)$ is odd. Therefore its regular part vanishes. To find the singular contribution, first note that

$$(\nabla_0^2+Dy)\,K\,\phi_0 = (K''-K^2)\,\phi_0 + 2K'\,\phi_0' + y\,(K'\,\phi_0 + K\,\phi_0') + K\,\phi_0$$

so that the integral becomes

$$i\int_{-\infty}^{+\infty}\left(\left(\frac{K-K^2+yK'}{U}+\frac{ic_1+K''}{U}\right)\phi_0^2 + \left(\frac{2K'+yK}{U}\right)\left(\frac{\phi_0^2}{2}\right)'\right)dy\,.$$

Since $K(0)=K(0)^2$ and $K'(y)/U(y)$ is regular, the only singular terms are

$$\int_{-\infty}^{+\infty} \frac{\phi_0^2}{U}\,(i\,c_1+K'')\,dy = \pm\, i\pi\,\phi_0^2(0)\,(i\,c_1+K''(0))\;\mathcal{R}\mathrm{es}\left(\frac{1}{U}\right)$$
$$= \pm\, i\pi\sqrt{\frac{\pi}{2}}\left(i\,c_1-\frac{2}{3}\right). \tag{3.37}$$

When choosing the branch for the integration, one takes the positive sign in the above expression whenever $U'(0) > 0$, as explained in Ref. 19, Section 8.5. Plugging (3.37) into (3.36) and using (3.35), then recalling that the disturbance is neutral and separating the real and imaginary part, one finds

$$c_1 = 0\,, \qquad a_1 = -\frac{4}{3}\left(\frac{\pi}{2}\right)^{\frac{3}{2}}\left(\int_{-\infty}^{+\infty}\phi_0^2(y)\,dy\right)^{-1} = -0.927\,. \tag{3.38}$$

Together with (3.32) and (3.35) this implies $c_{cr}(R)=0$ up to first order and

$$\alpha_{cr}(R) = 0.733 - \frac{0.863}{R} + \mathrm{O}\left(\frac{1}{R^2}\right). \tag{3.39}$$

IV. Numerical calculation of the neutral curve

While the limits of the neutral curve are determined from asymptotic analysis, numerical calculations have to be used in the intermediate parameter range. Prior to the description of the numerical method and the presentation of the results, a brief analysis of the arising eigenvalue problem is given. It will be argued that the symmetry of the shear layer profile brings about a simplification of the eigenvalue problem.

A. The eigenvalue problem for finding the neutral curve

The general eigenvalue problem, as defined by the fast decay requirement (2.10), and equations (2.9), can be treated as a standard, rather than a generalized eigenvalue problem. The equations can be combined into the following integrodifferential one

$$(\nabla_\alpha^2 + D\,y)\,\omega - i\,\alpha R\,(U - U''\,\nabla_\alpha^{-2})\,\omega = -i\,\alpha\,R\,c\,\omega\,. \tag{4.1}$$

Attention is now given to the spacial asymptotic behavior of the eigenfunctions and the way the properties of the mean shear flow $U(y)$ are reflected in the structure of the eigenvalue problem solutions. The asymptotic equation for $|y| \gg 1$ follows from (4.1) upon setting $U''(y)=0$ and $U(y)=U_{\pm\infty}$ where $U_{\pm\infty}=\lim_{y\to\pm\infty}U(y)=\pm 1$,

$$\omega'' + y\,\omega' + (1-\mu_\pm)\,\omega = 0\,, \qquad \mu_\pm = \alpha^2 + i\,\alpha\,R\,(U_{\pm\infty} - c)\,, \tag{4.2}$$

This equation has fast decaying solutions at both infinities. Neglecting the $U''(y)$ term is justified if it becomes asymptotically negligible compared to the $U(y)$ term. This is the case, for example, of any $\omega(y)$ decaying faster than $e^{-\alpha|y|}$ for $|y|\gg 1$ (then the latter function gives generally the asymptotic spatial decay rate of $\nabla_\alpha^{-2}\,\omega$) but no faster than the Gaussian. These two conditions assure that second term decays exponentially relatively to the first one; they

are met by the fast decaying solution to (4.2) and it can be therefore used to approximate the solution to (4.1) for large arguments. Note that (4.2) is exactly equation (B.2) in Appendix B. As it is mentioned there, a fast decaying solution to (4.2) is available on each half-axis, which is unique up to a constant multiple. The one for $y>0$ is given by (B.6) and that for $y<0$ is similarly defined. The asymptotic representation of these solutions (B.7) shows that their decay is of Gaussian type, so $\omega(y)$ is an α-fast decaying function on each half-axis (see for the definition Appendix C) for any value of α. This justifies the use of the form (C.2) instead of (C.1) for ∇_α^{-2}.

a. Odd profiles

It was probably for the first time in Ref. 10 that special attention was drawn to the fact that for odd velocity profiles the Orr-Sommerfeld equation has its complex eigenvalues coming in conjugate pairs. Betchov and Szewchyk[11] observed that numerically calculated eigenvalue problem solutions of the free shear layer Orr-Sommerfeld equation for an odd velocity profile (which was $\tanh(y)$ in their case but we found the same to apply for $\mathrm{erf}(y)$) the phase speed vanishes and the eigenfunctions can be always split into an even real and an odd imaginary part. In calculations for the Burgers vortex layer the same feature is observed, as mentioned by Lin and Corcos[7]. In preliminary computations on the same flow by a shooting method similar to that described in §IV.2 below, but assuming no symmetry for the eigenvalue problem solution, this feature was universally present.

To clarify the reason for this property of shear layer profiles, some general features are pointed out first. A linear operator will be called even, if it maps even functions into even ones and odd into odd ones; it will be called odd, if it maps even into odd and odd into even ones. Consider the operators $\mathcal{V}(y)=\nabla_\alpha^2+Dy=\mathcal{M}-\alpha^2$ and $\mathcal{U}(y)=U(y)-U''(y)\nabla_\alpha^{-2}$. Equation (4.1) can be written as $(\mathcal{V}+i\alpha Rc)\omega=i\alpha R\,\mathcal{U}\omega$. The operators Dy, ∇_α^2, ∇_α^{-2} are even; multiplication by an odd function like $U(y)=\mathrm{erf}(y)$ is an odd operator; $\mathcal{V}$ is even and $\mathcal{U}$ is odd: $\mathcal{V}(-y)=\mathcal{V}(y)$ and $\mathcal{U}(-y)=-\mathcal{U}(y)$. (For the free shear layer Orr-Sommerfeld equation the same is valid but with the different definition $\mathcal{V}=\nabla_\alpha^2$.) Note that $\mathcal{U}$ is a real operator: it maps real into real functions. The same holds for $(\mathcal{V}+i\alpha Rc)$ only if $c_r=0$. Generally, $(\mathcal{V}+i\alpha Rc)^*=\mathcal{V}-i\alpha Rc^*$. The observation in Ref. 10, which is also valid in the Burgers vortex layer problem, can be stated in the following way. Conjugating the eigenvalue problem equation, inverting the space direction $y\to -y$, and using that $\mathcal{V}(y)$ is even while $\mathcal{U}(y)$ is odd, one obtains from any eigenvalue problem solution $(c,\omega(y))$ another one, $(-c^*,\omega^*(-y))$. Only for eigenvalues with $c_r=0$ one has the same eigenvalue after the transformation. If such eigenvalues are simple, one may infer that under appropriate normalization $\omega(-y)=\omega^*(y)$, i.e. that $\omega_r(y)$ is even and $\omega_i(y)$ is odd.

Now *assume* that the most unstable modes are standing waves, $c_r=0$, so $(\mathcal{V}+i\alpha Rc)$ acts as a real, even operator on them, and their real and imaginary parts have the mentioned parity. The symmetry of the equation implies that such modes satisfy

$$\left((\alpha R)^{-1}\mathcal{V}-c_i\right)\omega_r=-\mathcal{U}\omega_i\,,\qquad \left((\alpha R)^{-1}\mathcal{V}-c_i\right)\omega_i=\mathcal{U}\omega_r\,, \tag{4.3}$$

which puts a real eigenvalue problem. The assumption is justified in view of the mentioned observation that the Orr-Sommerfeld eigenvalue problem for odd profiles gives numerically $c_r = 0$, and in view of the results of the asymptotic analysis presented here, which show that, to the considered order, $c = 0$ on the neutral curve.

b. Real eigenvalue problem

The construction of a solution defined only on one half-axis is possible due to the fact that the tentative solutions have asymptotic behavior which assures them to be α-fast decaying, and then ∇_α^2 is invertible on them over any half-infinite interval.

A fast decaying solution to (4.3) on the negative half-axis can be constructed by taking, for example, $\omega_r(y) = \omega_r(|y|)$ and $\omega_i(y) = -\omega_i(|y|)$, i.e. the real and imaginary parts are reflected as an even and an odd function, respectively. The obtained function has to be a global solution to (4.3), so $\phi(y)$ and $\omega(y)$ must be matched smoothly at the origin.

Assume there exists a fast decaying global solution with $\omega_r(y)$ even and $\omega_i(y)$ odd. As can be seen from Appendix C the operator ∇_α^2 preserves this parity, and one has

$$\phi_r'(0) = 0, \qquad \phi_i(0) = 0, \qquad \omega_r'(0) = 0, \qquad \omega_i(0) = 0. \tag{4.4}$$

This is enough, in principle, to write down a secular condition (in terms of the values at the origin of a couple of linearly independent functions $\omega_j(y)$, $\phi_j(y)$, $j = 1, 2$, satisfying (4.1) on one half-axis) that defines implicitly the eigenvalue $c_i(\alpha, R)$. In practice, however, it proves a better choice to incorporate more of the solution structure in the secular condition. On the positive half-axis the representation (C.2) from Appendix C can be used for $\phi(y)$, that is,

$$\phi(y) = (\nabla_\alpha^{-2}\omega)(y) = \int_{+\infty}^{y} \frac{\sinh(\alpha(y-y_1))}{\alpha}\,\omega(y_1)\,dy_1 - E^+ e^{-\alpha y}. \tag{4.5}$$

To determine the constant E^+, use (C.4) and require that $\omega_r(y)$ be even and $\omega_i(y)$ be odd, to find that $E^- = (E^+)^*$; this and the eigenfunction symmetry imply that (C.4) is equivalent to

$$\mathcal{R}e\, E^+ = \int_0^{+\infty} \frac{\cosh(\alpha\, y)}{\alpha}\,\omega_r(y)\,dy, \qquad \mathcal{I}m\, E^+ = \int_0^{+\infty} \frac{\sinh(\alpha\, y)}{\alpha}\,\omega_i(y)\,dy, \tag{4.6}$$

Using (4.5) and (4.6) to evaluate $\phi(0)$ and $\phi'(0)$, one may now put the symmetry requirement for $\omega(y)$ in the equivalent form

$$\phi_r(0) = \int_{+\infty}^{0} \frac{e^{-\alpha y}}{2\alpha}\,\omega_r(y)\,dy, \qquad \phi_i(0) = 0, \qquad \omega_r'(0) = 0, \qquad \omega_i(0) = 0. \tag{4.7}$$

Starting with two different E^+ from $+\infty$ and integrating (4.1) toward the origin produces two independent solutions defined on the positive half-axis. A linear combination $\phi = c_1\phi_1 + c_2\phi_2$ corresponds to $\omega = c_1\omega_1 + c_2\omega_2$ and to $E^+ = c_1E_1^+ + c_2E_2^+$. One seeks complex numbers c_1 and c_2 such that the corresponding combinations satisfy the conditions (4.7). There are four real parameters that must satisfy a set of four real homogeneous linear equations. The determinant of the resulting system must vanish, which gives a single, real algebraic condition that relates implicitly the eigenvalue c_i to the parameters R and α.

In this way, the assumption of standing wave solutions leads to a real eigenvalue problem for the growth rate αc_i. On the neutral curve the latter vanishes, and one is left with a relation between R and α. This defines a real eigenvalue problem, with the eigenvalue given either by $R(\alpha)$ or by $\alpha(R)$.

B. Numerical method

A classical shooting method was apllied for the numerical calculations. It uses the symmetry of the profile to calculate directly the neutral curve as explained in §IV.1, but a simple modification allows the calculation of damped and growing modes as well.

For the numerical integration a fourth-order Runge-Kutta scheme was used. The stepsize was decreased until a 6-digit agreement was assured for the eigenvalue. The governing equation is put in canonical form by introducing a four-dimensional complex vector (f_0, f_1, f_2, f_3) such that the streamfunction and vorticity are $\phi(y) = f_0(y)$, $\omega(y) = \phi'' - \alpha^2 \phi = f_2(y)$, and

$$f_0'(y) = f_1(y), \qquad f_1'(y) = f_2(y) + \alpha^2 f_0(y), \qquad f_2'(y) = f_3(y),$$
$$f_3'(y) = (\alpha^2 - 1) f_2(y) - y f_3(y) + i\alpha R (U(y) f_2(y) - U''(y) f_0(y)).$$

Numerical integation is started at some point y_0, far enough from the origin, such that both $|U''(y_0)|$ and $1 - |U(y_0)|$ are small. (For $U(y) = \mathrm{erf}(y)$, taking $y_0 = 4, 6, 8$ gives 1×10^{-3}, 7×10^{-8}, 8×10^{-14}, and 6×10^{-5}, 2×10^{-9}, 1×10^{-15}, respectively.) The values of $\omega(y_0)$ and $\omega'(y_0)$ are computed using the exact form (B.6) of the fast decaying solution of (4.2). For $\phi(y_0)$ and $\phi'(y_0)$, the integral representation (4.5) is used, with "actual infinity" at $2y_0$ say; there $\omega(y)$ is well approximated by (4.5), and numerical integration is no problem, provided the integrand is not highly oscillatory, which excludes $\alpha R \gg 1$. A second independent solution is generated simultaneously, starting from an initial condition for $\phi(y_0)$ and $\phi'(y_0)$ with a homeogeneous solution component added: $E e^{-\alpha |y_0|}$ and $-\alpha E e^{-\alpha |y_0|}$ respectively.

There are some natural limitations on the applicability of the shooting method. For a correct computation at small wavenumbers, a longer shooting distance y_0 is required, because of the rather slow decay rate (4.5) of the streamfunction. For large Reynolds numbers the definition (4.2) suggests that $|\mu(\alpha, R)| \propto R$ and the asymptotic form (B.7) of the solution for $\omega(y)$ has an algebraic prefactor oscillating with an $O(1/\log(R))$ spacial period (cf. (B.7)). Strictly speaking, the asymptotic expansion for $\omega(y)$ is valid, and the function itself is fast decaying, only for $|y| > |\mu|$, i.e. beyond an increasing y_0. In practice, however, the faster exponential growth of roundoff error ("stiffness") requires fewer steps and a shorter shooting distance for the computations with growing Reynolds number, while the distance y_0 is limited from below by the size of the region in which the profile signifficantly differs from its asymptotic value, approximately $y_0 = 4$. (In the range $20 \leq R \leq 40$ the appropriate shooting distance is about 4, while for $0.001 \leq \alpha \leq 0.1$ it is about 8. The maximum Reynolds number for which the integration is reliable, is about 40, while the upper limit in the wavenumber is about 0.71. The latter is understood as the value corresponding to the maximum Reynolds number, that can be reached. Note that the critical wavenumber, above which no inviscid solution exists, is $\alpha_{cr} \approx 0.73$.)

In the "inviscid case" $1/R=0$ the Rayleigh equation $(U(y)-c)(\phi''-\alpha^2\phi)-U''(y)\phi=0$ must be solved, which allows for only one decaying solution on each half-axis. Since $U''(y)$ is fast decaying, the eigenfunction must decay like $e^{-\alpha|y|}$. An inviscid neutrally stable mode corresponds to a real eigenvalue problem for the wavenumber, as discussed in §III.2. The eigenvalue controls the dacay rate of the eigenfunction. A shooting procedure similar to the one described above is used in this case, as well. Differentiating once the asymptotics for large y provides the initial condition for ϕ'. The second-order, real system is integrated numerically only over the positive half-axis, then $\phi'(0)=0$ is solved. The eigenfunction is readily produced by recording the result at each Runge-Kutta step; this allows the calculation of $\int_{-\infty}^{+\infty}\phi_{cr}^2(y)\,dy$ which is used in §III.2.

C. Results from numerical computations

The neutral curve calculation is the main result of this paper (see Fig. 2(a)). Most interesting is the critical Reynolds number region shown in Fig. 2(b). The thick curve represents the numerical approximation to the neutral curve, the dotted line indicates the first-order asymptotic approximation (3.24) to the curve for small wavenumbers, and the dashed line shows the first-order asymptotic approximation (3.39) for large Reynolds numbers. The latter approximation remains close to the numerical results over their whole range.

The shooting method applied here allows for a fairly precise calculation of the neutral curve for small wavenumbers (6 digits for $\alpha<0.5$). Numerical results for some typical values of either the Reynolds number or the wavenumber are listed in Table 1. A comparison can be made with the linear growth-rate computations of Lin and Corcos [7]. (We note in passing that equation (4.1) given there has typing error in the term due to strain.) The length scale chosen there is $\sqrt{\pi/2}$ times larger than the presently used one, so it is to be expected that the zero crossings of growth-rate curves shown on Figure 16 there give $\alpha_{cr}(R)$ times the mentioned factor. Allowing for an error of the order of 1%, one obtains for $R=5,10,20,\infty$ respectively $\alpha=0.53,0.63,0.69,0.73$ which are to be compared with 0.57, 0.65, 0.69, and 0.73, obtained by the present method. It should be noted that an increasing discrepancy is found when the Reynolds number falls below 20 and that no data are available[7] for $R<5$.

The present result allows to conclude that indeed a finite critical Reynolds number exists, $R_{cr}=1$. It is obtained at the small-wavenumber end of the neutral curve, and no lower branch exists, at least for standing wave normal modes. The numerical curve is strictly monotonic and either of α or R can be taken as independent parameter to parametrize the whole curve. The inviscid limit gives the upper bound for the wavenumbers of the neutral disturbances, just as in the case of free shear layers.

It is not well understood why (3.39) gives a good approximation to the neutral curve even at the small-wavenumber end, but one may argue plausibly as follows. In the large-Reynolds-number limit, one finds using (3.35) that $\omega''(0)=-1.13$ while $\left(e^{-y^2/2}\right)''\Big|_{y=0}=-1$ which suggests that $\omega(y)$ is close to the Gaussian around the origin, while both functions have comparable decay rates for large arguments (see (3.27) and note that $K(y)\propto ye^{-\frac{1}{2}y^2}$). In fact such closeness is observed for all Reynolds numbers and means that the variation of $\alpha\phi_r(0)$ is

relatively small (see the first equation in (4.7)).

As an illustration of the neutral modes, the vorticity of the inviscid eigenfunction, which is real, and of a typical case of a small-wavenumber mode are represented in Figures 4 and 5 respectively, the normalization being $\phi_r(0) = -1$ (compare with (3.15) which is also used in § III.2). The real part of the vorticity remains a fast decaying function well approximated by the Gaussian, for all neutral modes (compare Fig. 4 and Fig. 5). For small Reynolds numbers the reason is that the part of the Orr-Sommerfeld equation due to viscosity and strain is given by the Hermite operator $\mathcal{M}$ (see (3.7) and (3.5)). Indeed, the shape remains virtually unchanged when $\alpha \to 0$ and agrees with that of the leading-order solution components obtained from small-wavenumber asymptotics, which are plotted with dotted lines in Fig. 5 and are practically indiscernible from the ones computed for $\alpha = 0.1$. For large Reynolds numbers, it is due to the Gaussian type decay of $U''(y)$ for large arguments, which in turn stems from the fact that the stationary Burgers vortex layer itself has its vorticity governed by the Hermite operator. The imaginary part of vorticity decreases monotonously (figures omitted) with increasing Reynolds number, remaining an odd function similar in shape to that in Fig. 5.

The uniformity of the shape of ω_r is specific to the current problem. It would not be the case if $U''(y)$ were to decay much more slowly than the Gaussian. The leading-order solution in the small-wavenumber limit would generally be given by $\omega(y) = h_0(y) - i\,R_0\,(D^2 + Dy)^{-1}\,U''$ for $U''(y)$ odd and decaying and $\int_{-\infty}^{+\infty} U'(y)\,dy = 2$. The imaginary part would have roughly a decay rate of $U''(y)$. Even with the same profile, however, in the absence of the external strain field the small-wavenumber limit of the neutral curve is substantially different. It is shown in Appendix A that this is related to the vanishing spatial decay rate of $\omega(y)$ in this limit. The shape of the disturbance changes essentially along the neutral curve — while in the large-Reynolds-number limit it is governed by the Rayleigh equation, which is the same in the case with strain, it tends to the shape of the basic velocity profile as $\alpha \to 0$.

V. Concluding remarks

We have calculated the whole neutral curve for the two-dimensional linear stability of the Burgers vortex layer, which is an exact stationary solution to the Navier-Stokes equations representing a viscous shear layer stabilized by a two-dimensional stagnation-point flow. The previously known existence of a positive critical Reynolds number[8,15] has been confirmed in a rather different setting.

In these earlier studies, the dynamics of the vortex layer is reduced respectively to that of a single scalar[8], namely the overall shear across the layer at a fixed streamwise location, which is the zeroth-order moment of vorticity in the spanwise direction, and to a system for the first three momenta[15]. Using the coordinates introduced in Sec. II, we note that in both cases it is assumed that the disturbance comprises an x-dependent modulation and local deviation from the y-axis of the stationary Burgers vortex layer, given by the Gaussian vorticity profile. In Ref. 8 the deviation is taken to depend explicitly on the modulation of the layer strength. In Ref. 15 the local (along the x-direction) lengthscale in the y-direction of the layer. i.e. the layer

thickness, is also perturbed, but its shape is still a Gaussian in y. A larger lengthscale then means a flatter vorticity distribution but leaves its integral along the whole y-axis unchanged. To relate these settings with the present one, we note that only odd Orr-Sommerfeld modes contribute to the deviation of the centerline of the vortex layer from its equilibrium position, only the even modes with non-zero integral (over the whole y-axis) contribute to the variation of the layer strength, and the rest (if present) contributes only to the variation of the layer lengthscale in y. At least for the neutral modes found here (as well as for the damped or growing modes with even real and odd imaginary parts which we have found via a modification of the shooting method described in §IV.2), the spatial extent in the y-direction is effectively that of the undisturbed layer, for all wavenumbers. This means that the deviation of the disturbance from the centerline is confined within the layer thickness, and that the deviation of the whole vortex layer is first-order small in the disturbance amplitude. Moreover, the (imaginary) odd components of the vorticity disturbances tend to zero with increasing Reynolds number, and the same then applies to the layer displacement. Using its definition given by Passot *et al.*[15] in terms of vorticity momenta, one finds that the variation in the y-lengthscale is also first-order small in the amplitude. The solution given in §III.1 shows further that it is second-order small in the wavenumber.

In the stability analysis adopted here, amplitude linearization is performed at the outset, without any assumption about the shape of the disturbances. In the treatment adopted in the other two papers, a small-wavenumber linearization is first made (the streamwise lengthscale of the disturbance is taken very large compared to the layer thickness), then assumptions on the shape of disturbances are used to obtain some nonlinear equations. Thus, the present description accounts for disturbances nonlinear only in the wavenumber, while that in Ref. 8,15 retains disturbances nonlinear only in amplitude. Therefore, results are comparable only when the linearizations of the nonlinear equations, as given in those papers, and the limit of small wavenumbers, as given here, are taken. The one-dimensional problem considered by Neu[8] correctly recovers the critical Reynolds number, corresponding to the only neutrally stable mode found here when $\alpha=0$ (cf. the leading-order solutions discussed in §III.1). The system of third order[15] recovers in the same limit the first three eigenfunctions with $\lambda=0,-1,-2$. The slopes of the neutral curves for these problems are given by $R_1=2/\sqrt{\pi}$, after adjusting the scalings of Neu[8] to the presently used ones, and $R_1=1/\sqrt{\pi}$, in the case considered by Passot *et al.*[15]. A problem closed for the zero and first-order momenta of vorticity (no local layer thickness variation) can be derived in an analagous way; it recovers the eigenvalues $\lambda=0,-1$ as expected, but gives $R_1=1/(4\sqrt{\pi})$. On the other hand, the value obtained here is $3/\sqrt{\pi}$ (see (3.24)).

We calculate the critical Reynolds number for the Burgers vortex layer from an Orr-Sommerfeld eigenvalue problem. It is verified that this is indeed a small-wavenumber phenomenon. It is expected to be independent, to leading order, of the exact shape of the vortex layer. If another odd monotonous profile is taken instead of $U(y)=\mathrm{erf}(y)$ (and is assumed to be stationary, although no corresponding solution of the Navier-Stokes equations exists — this is the same procedure as in the linear stability analysis of a free shear layer which, strictly

speaking, cannot be stationary), a similar result is obtained in the small-wavenumber limit. The unstable modes at Reynolds numbers larger than the critical are expected to have spatial lengthscale (in both x- and y-direction) of the order of the layer thickness, although their shape will be sensitive to the basic flow form, e.g. $\omega_i(y) \propto U(y)$ when $\alpha \to 0$. For large Reynolds numbers the instability is essentially of the Kelvin-Helmholtz type, very similar to that of the free mixing layer of finite thickness and with the same short-wave cutoff. The inviscid asymptotics is found to furnish an approximation to the neutral curve which remains good for all Reynolds numbers. This is related to the fact that the vorticity disturbance remains well localized (accross the layer) for all Reynolds numbers, with a spatial decay rate comparable to that of the basic flow vorticity. The shape of neutrally stable Orr-Sommerfeld eigenfunctions is shown to have specific symmetry due to the symmetry of their basic flow. Numerically computed shapes agree with the (explicit) leading-order asymptotic approximation in the small-wavenumber limit.

No growth-rates are presented here, although a shooting method similar to the one used here was found to be a reliable means for obtaining them even far from the neutral curve, for the case of Burgers vortex layer profile, in the range $R < 40$ and $\alpha < \alpha_{cr} = 0.733$. Data for $R \geq 5$ are given for the Burgers vortex layer by Lin and Corcos[7], and for a free mixing layer with a hyperbolic tangent and an error function profile by Betchov and Szewchyk[11] and Sherman[16], respectively.

The linear two-dimensional normal mode stability analysis of the stationary Burgers vortex layer is only a minor first step. One would like to have more results concerning three-dimensional, linear and finite amplitude disturbances, to include the general case of three-dimensional irrotational strain (for the case of single axis of stretching, stationary elliptic tubes have been found[9], but there exist also vortex layer solutions), as well as the effects of rotational strain and curvature. The existence of time-dependent self-similar solutions tending to the Burgers vortex layer (see Ref. 16, p.155) and the Burgers vortex tube (see Ref. 16, p.466, and Ref. 17, p.272), which model the relaxation of a more localized or spread-out vorticity configuration toward the equilibrium state given by the Burgers solutions, calls for an appropriate study of their stability, especially for early times. Very recently[20] a whole family of stationary solutions to the Navier-Stokes equations was discovered, representing arrays of spanwise vortices, periodic in the streamwise direction, and invariant in the spanwise direction, which are maintained by the same two-dimensional stagnation-point flow as the Burgers vortex layer. They may be the right cadidates for equilibrium solutions at higher Reynolds numbers, when the Burgers vortex layer becomes linearly unstable.

Appendix A Free shear layer neutral modes

For a better understanding of the effect of irrotational strain, hereafter the linear stability of strained shear layer is compared to that of a free shear layer. As before, we consider standing waves, $c = 0$; it is argued in §IV.1 that this is a general feature of parallel flows with mean velocity pofile given by an odd function. The Orr-Sommerfeld equation can be put in the form

$$\nabla_\alpha^2 \omega - i\alpha R(U - U''\nabla_\alpha^{-2})\omega = 0, \qquad \nabla_\alpha^2 = D^2 - \alpha^2, \tag{A.1}$$

which is to be compared with (4.1) for the case with strain. Its asymptotic form for large arguments, when $U(y)\to U_{\pm\infty}=\pm 1$ as $y\to\pm\infty$, is $\omega''-\mu_\pm\omega=0$ with $\mu_\pm=\alpha^2-i\alpha R U_{\pm\infty}$. A decaying solution has a leading-order asymptotic form

$$\omega(y)\approx C_\pm \exp\left(-|y|\sqrt{\mu_\pm}\right)=C_\pm \exp\left(-\alpha\varphi_\pm(\rho(\alpha))|y|\right), \quad \pm y\gg 1, \tag{A.2}$$

$$C_\pm=\text{const.}, \qquad \rho(\alpha)=\frac{R(\alpha)}{\alpha}, \qquad \varphi_\pm(\rho)=\sqrt{1\pm i\rho}, \quad \mathcal{R}e\,\varphi_\pm>0. \tag{A.3}$$

Its amplitude is bounded by $|C_\pm|\,e^{-\alpha\varphi_r(\rho)|y|}$, $\varphi_r=\mathcal{R}e\,\varphi_\pm(\rho)=\cos\left(\frac{1}{2}\arctan(\rho)\right)(1+\rho^2)^{1/4}$. The function $\varphi_r(\rho)$ grows monotonously from 1 to $+\infty$ when ρ is increased from 0 to $+\infty$. Inspection of the neutral curve[12] shows that R/α is uniformly bounded above zero, so $\varphi_r(\rho)>1$. This is an *a posteriori* confirmation of the α-fast decaying property of $\omega(y)$ in the case of free shear layer, which justifies the use of the asymptotic form of the Orr-Sommerfeld equation (see Appendix C and §IV.1).

a. Small-wavenumber asymptotics

It is known[10] that in the small-wavenumber limit the critical curve for a free shear layer with odd profile $U(y)$ is given by $R(\alpha)=4\sqrt{3}\,\alpha+O(\alpha^3)$ where the higher order corrections depend on the profile. The shape of the eigenfunction, however, has not been calculated in that limit explicitly, at least to our knowledge. For $\alpha\ll 1$ the tail of $\omega(y)$ has a dominant contribution to $\phi(y)=\nabla_\alpha^{-2}\omega$, or explicitly, $-1/(2\alpha)\int_{-\infty}^{+\infty}e^{-\alpha|y-y_1|}\omega(y_1)\,dy_1$. Inserting the asymptotic form (A.2) in the integral introduces an $O(1)$ error, while the contribution from the tails is $O(\alpha^{-1})$. Noting also that $e^{-\alpha|y-y_1|}=e^{-|\alpha y_1|}+O(\alpha)$, one may evaluate the integral to leading order, $\phi(y)=(1/\alpha^2)\left(-\int_0^{+\infty}e^{-y_1}\frac{1}{2}\left(C_+e^{-\rho_+(\varphi(\alpha))y_1}+C_-e^{-\rho_-(\varphi(\alpha))y_1}\right)dy_1+O(\alpha)\right)$. The eigenfunctions $\omega(y)$ and $\phi(y)$ will be taken normalized as in §IV.1 with their real parts even and their imaginary parts odd. Then $C_-=C_+^*$, $\varphi_-=\varphi_+^*$, and the imaginary part of the integral vanishes; its real part is given by $\mathcal{R}e(C_+/(\varphi_+(\rho)+1))$. Denoting $\varphi_r=\mathcal{R}e\,\varphi_+(\rho)$, and $\varphi_i=\mathcal{I}m\,\varphi_+(\rho)$, $C_r=\mathcal{R}e\,C_+$ and $C_i=\mathcal{I}m\,C_+$, one evaluates this expression as $C(\rho)/\rho$ where $C(\rho)=C_i(\varphi_r-1)+C_r\varphi_i$. The obtained leading-order form of $\phi(y)$ can be substituted into the governing equation, to find the leading-order terms in α, namely $\omega''=i\rho U''(-\alpha^2\nabla_\alpha^{-2}\omega)+O(\alpha^2)=iU''C(\rho)+O(\alpha)$. In the limit $\alpha\to 0$ for fixed y, one finds $\omega_r(y)\to 0$ and $\omega_i(y)\to C(\rho)U(y)$, so that $C_r=0$ and $C_i=1$, with $\rho\to\rho(0)$ such that $C(\rho(0))=C_i$. This is equivalent to $\varphi_r(\rho(0))=2$ with solution $\rho(0)=4\sqrt{3}$.

To summarize, the neutral modes in the small-wavenumber limit differ signifficantly between the cases with and without irrotational strain. This is due to the fact that the decay rate of $\omega(y)$ for $|y|\to+\infty$ with α fixed, which is given in (A.2), vanishes with α. In contrast, the leading-order solution (3.14) has a Gaussian decay. The limit of $\omega(y)$ when $\alpha\to 0$ for fixed y is given by $iU(y)$. In the strained case, it is $h_0(y)+i\mathcal{M}^{-1}U(y)$, a fast decaying solution. In both cases it is essential that $U(y)$ is odd.

b. Large-Reynolds-number asymptotics

The analysis for large Reynolds numbers is a repetition of the one already given in § III.2 except for one minor difference. The term due to the irrotational strain is absent, so the first-order solvability condition, with $c_1 = 0$, changes from (3.36) to

$$0 = a_1 \int_{-\infty}^{+\infty} \phi_r^2 \, dy \; + i \int_{-\infty}^{+\infty} \frac{\phi_r(y)}{U(y)} \nabla_0^2 \, (K \, \phi_r) \, dy \, . \tag{A.4}$$

The second integral is rewritten as $i \int_{-\infty}^{+\infty} \left(\left((K'' - K^2) / U \right) \phi_r^2 \; + \; (K'/U) \, (\phi_r^2)' \right) dy$, and the singular part, to be compared with (3.37), is given by $\int_{-\infty}^{+\infty} \phi_r^2 \, (K'' - K^2) / U \, dy = -\frac{5}{3} \, i\pi \sqrt{\frac{\pi}{2}}$. The leading-order result remains unchanged, so the limiting shape of the eigenfunctions is the same in the cases with and without irrotational strain. At first order, in the case of free shear layer with $U(y) = \mathrm{erf}(y)$, (3.38) becomes $a_1 = -\frac{10}{3} \, (\frac{\pi}{2})^{\frac{3}{2}} \left(\int_{-\infty}^{+\infty} \phi_r^2(y) \, dy \right)^{-1} = -2.3175$, and (3.39) is modified as $\alpha(R) = 0.733 - 2.157/R + \mathrm{O}(R^{-2})$. Thus the strained shear layer is *linearly less stable* than the free shear layer at high Reynolds number, in the sense that growing disturbances exist for a wider range of wavenumbers.

Appendix B Gaussian and related functions

The version of the Gaussian function h_0 used in this paper is normalized to obtain the error function simply as

$$\mathrm{erf}(y) = h_{-1}(y) = \int_0^y h_0(y_1) \, dy_1 \, , \qquad\qquad h_0(y) = \sqrt{2/\pi} \, \exp\left(-y^2/2\right) \tag{B.1}$$

These functions present the vorticity and parallel flow velocity profiles considered in this paper. Related functions that occur in the analysis are considered below and in Appendix D.

a. Hyperbolic cylinder equation

With the substitution $\omega(y) = f(y) \exp(-y^2/4)$ the equation

$$\mathcal{M} \, \omega = \mu \, \omega \tag{B.2}$$

associated with the Hermite differential operator defined in (3.5), can be transformed into the hyperbolic cylinder equation (see Ref. 21, Sec.19.1),

$$f'' - \left(\frac{y^2}{4} - \frac{1}{2} + \mu \right) f = 0 \tag{B.3}$$

The solution of (B.2) for general μ is a linear combination of the odd and even solutions of that equation which are found from the corresponding solutions of (B.3) (see Ref. 21, Sec.19.2), and have the form

$$\omega_1(y) = \exp\left(-\frac{y^2}{2}\right) \, y \, M\left(\frac{\mu+1}{2}, \frac{3}{2} \, ; \, \frac{y^2}{2}\right) , \qquad \omega_2(y) = \exp\left(-\frac{y^2}{2}\right) \, M\left(\frac{\mu}{2}, \frac{1}{2} \, ; \, \frac{y^2}{2}\right) \tag{B.4}$$

From the asymptotics of the confluent hypergeometric function $M(a,b\,;z)$ for large z given in Ref. 21, Sec.13.5, it follows when $z=-y^2/2$ that the general case of large argument asymptotics for the present case is

$$\omega_1 \propto |y|^{\mu-1}, \quad \mu\neq -1,-3,-5,\ldots, \quad \omega_2 \propto |y|^{\mu-1}, \quad \mu\neq 0,-2,-4,\ldots, \quad y^2\gg|\mu| \tag{B.5}$$

However, a separate fast decaying solution always exists on each half-axis, and both its explicit form (see Ref. 21, 19.12.3) and its asymptotics for large arguments (See Ref. 21, 19.8.1) are available. For $y>0$ one has

$$\omega(y)=e^{-\frac{y^2}{2}}\frac{\sqrt{\pi/2}}{2^\mu}\left(\frac{1}{\Gamma(\frac{\mu+1}{2})}\,M\left(\frac{\mu}{2},\frac{1}{2}\,;\,\frac{y^2}{2}\right)-\frac{\sqrt{2}}{\Gamma(\frac{\mu}{2})}\,y\,M\left(\frac{\mu+1}{2},\frac{3}{2}\,;\,\frac{y^2}{2}\right)\right), \tag{B.6}$$

$$\omega(y)\approx e^{-\frac{y^2}{2}}\,y^{-\mu}\sum_{n=0} a_n\left(-2/y^2\right)^n, \qquad a_n=\prod_{j=0}^{n}(j+\mu), \tag{B.7}$$

and for $y<0$, $|y|\gg 1$, one adds instead of substracting, the second term in (B.6) and takes $|y|^{-\mu}$ instead of $y^{-\mu}$ in (B.7). These representations are formally valid for $\mu=0,-1,-2,\ldots$ if the limit is taken in (B.6) is replaced by its limit. One of the terms in (B.6) vanishes and the other is given by a finite series. This leads to the family of fast decaying functions defined on the real axis, called *Hermite functions* in this paper. (The common usage of this name refers to functions greater that the presently used by const. $e^{y^2/4}$.)

b. Hermite functions

In the asymptotic analysis we use the Hermite functions

$$h_n(y)=D^n h_0(y), \qquad n=0,1,2,\ldots, \qquad\qquad \mathcal{M}h_n=-n\,h_n, \tag{B.8}$$

where the *Hermite operator* $\mathcal{M}=D^2+yD+1$ is defined in (3.5). The second equation in (B.8) follows inductively from the first by noting that $D\mathcal{M}D^n=(\mathcal{M}+1)D^{n+1}$. The eigenvalue problem posed by the first equation when it is only required that the eigenfunction be in $L_{2(-\infty,+\infty)}$, has always two solutions. One of these is h_n which decays faster than exponentially and is even/odd if $-n$ is even/odd. The other decays like $y^{-(n+1)}$ and is odd/even, i.e. of opposite parity. If at least exponential decay (2.10) is required, only the $h_n(y)$ remain. The normalization (B.1), decay and (B.8) imply

$$\int_{-\infty}^{+\infty} h_0(y)\,dy=2, \qquad \int_{-\infty}^{+\infty} h_0^2(y)\,dy=\frac{2}{\sqrt{\pi}}, \qquad \int_{-\infty}^{+\infty} h_n(y)\,dy=0, \quad n=1,2,\ldots \tag{B.9}$$

We need to specify the form and asymptotic of the "slow" eigenfunction only for $n=0$. It is also called the *Dawson integral* (see Ref. 21, section 7.1). Its properties can be found from those of hyperbolic cylinder functions (see Ref. 21, sections 19.8, 19.14), ever multiplying by $\sqrt{\pi/2}\exp(-y^2/4)$. Its definition and large y asymptotics are

$$\mathcal{D}(y) = h_0(y)\int_0^y h_0(y_1)^{-1}\,dy_1=\exp(-y^2/2)\int_0^y \exp(y_1^2/2)\,dy_1 \tag{B.10}$$

$$\mathcal{D}(y) = \frac{1}{y}+\frac{1}{y^3}+O\left(\frac{1}{y^5}\right), \qquad |y|\gg 1 \tag{B.11}$$

c. Inhomogeneous Hermite equation

Any second-order differerential operator of the form $A = D^2 + a(y)D + b(y)$ defines a homogeneous ordinary differential equation $Af = 0$ which has always two linearly independent solutions. The Wronskian of any two solutions of the homogeneous ODE is

$$\mathcal{W}(f_1, f_2; y) = f_1' f_2 - f_1 f_2' = \text{const.} \exp\left(-\int_{y_0}^{y} a(y_1)\, dy_1\right). \tag{B.12}$$

For integrable $a(y)$ linear independence at any finite y_0 extends to all y. Given $f_1(y)$ and $f_2(y)$ and thus also $\mathcal{W}(y)$, the general solution of the inhomogeneous equation $Au = g(y)$ is found in the general form

$$u(y) = f_1(y) \int_{y_0}^{y} \frac{f_2(y_1)}{\mathcal{W}(y_1)} g(y_1)\, dy_1 - f_2(y) \int_{y_0}^{y} \frac{f_1(y_1)}{\mathcal{W}(y_1)} g(y_1)\, dy_1 + C_1 f_1(y) + C_2 f_2(y) \tag{B.13}$$

where the constants C_1, C_2 are determined by the boundary data. In the particular case $A = \mathcal{M}$ one takes $f_1(y) = \mathcal{D}(y)$ and $f_2(y) = h_0(y)$, so $\mathcal{W}(y) = h_0(y)$. The solution of $\mathcal{M}u = F(y)$ can be expressed using (B.10) and $y_0 = 0$ as

$$u(y) = h_0(y) \left(\left(\int_0^y F(y_1)\, dy_1 \right) \left(\int_0^y \frac{1}{h_0(y_1)}\, dy_1 \right) - \int_0^y dy_1\, F(y_1) \int_0^{y_1} \frac{1}{h_0(y_2)}\, dy_2 \right) + C_1 \mathcal{D}(y) + C_2 h_0(y).$$

Consider $F(y) = f'(y)$ with $f(y)$ bounded, smooth, and such that $f(y) - f_\infty$ is localized, for some suitable constant f_∞, in the sense that it is fast decaying at both infinities. Any fast decaying solution is then given by

$$\mathcal{M}u = \frac{\mathrm{d}}{\mathrm{d}y} f(y) \qquad u(y) = h_0(y) \left(\int_0^y \frac{f(y_1) - f_\infty}{h_0(y_1)}\, dy_1 + C_2 \right) \tag{B.14}$$

with $C_1 = f_0 - f(\infty)$, so the slowly decaying parts cancel out.

While (B.14) gives explicitly any *local* solution to the inhomogeneous Hermite equation, considering the problem on the whole real axis with decay condition (2.10) implies the solution must be in $L_{2(-\infty,+\infty)}$. Then the solvability condition must be satisfied, requiring that the right hand side is orthogonal to the kernel of the conjugate operator. The formal conjugate of the Hermite operator is $\mathcal{M}^* = (D - y)D$, its pairs of eigenvalues and eigenvectors under suitable boundary conditions are $-n$ and the Hermite polynomials $H_n(y) = e^{\frac{y^2}{2}}$, $n = 0, 1, 2, \ldots$. Because $H_0 = 1$, the solvability condition for (B.14) takes the form

$$\int_{-\infty}^{+\infty} F(y)\, dy = 0 \qquad \text{for} \qquad \mathcal{M}u = F, \tag{B.15}$$

assuming $(u'(y) + y\, u(y))\big|_{y=-y_\infty}^{+y_\infty}$ decays as $y_\infty \to \infty$. Since $u(y)$ solves a second-order ODE, it has differentiable asymptotics and it is sufficient if it decays faster than y^{-1}. (In the cases where (B.15) is applied in this paper, it is verified that the solution is in fact decaying faster than exponentially.)

Appendix C Inverse of the Laplacian

The ordinary differential operator ∇_α^2 defined in (2.8) is shown to be invertible on $L_{2(-\infty,+\infty)}$ and the explicit form of its inverse is given, along with the formal expansion of that integral operator for small wavenumbers α. While the general form of the inverse is valid for any locally integrable and bounded function defined on the real axis, it has the drawback that it requires the knowledge of the function over the whole axis. For fast decaying functions an alternative formula is valid, which requires only knowledge of the function between the point of interest and the positive or negative infinity. Note that ∇_α^2 maps even functions into even ones, odd into odd ones. Any (smooth, decaying) function uniquely decomposes into (smooth, decaying) even and odd components. It follows that the inverse operator, denoted ∇_α^{-2}, posesses the same property.

All homogeneous solutions of $\nabla_\alpha^2 u = 0$ are growing at $-\infty$ or $+\infty$, so ∇_α^2 is uniquely invertible for bounded functions. Using the Green function for ∇_α^2, a general explicit form of its inverse which gives a solution to $\nabla_\alpha^2 u = g(y)$ for any bounded continuous $g(y)$, is written as

$$(\nabla_\alpha^{-2}\, g)(y) = -\frac{1}{2}\int_{-\infty}^{+\infty} \frac{\exp\left(-\alpha\,|y-y_1|\right)}{\alpha}\, g(y_1)\, dy_1\,. \tag{C.1}$$

If $g(y)$ is a decaying function at infinity, so is $\nabla_\alpha^{-2}\, g$, and if $g(y)$ is decaying in a manner slower than $\exp\left(-\alpha\,|y|\right)$, so does $\nabla_\alpha^{-2}\, g$ but if it is decaying faster, then the inverse is generally decaying only like $\exp\left(-\alpha\,|y|\right)$.

a. Volterra integral form for fast decaying functions

For fixed $\alpha > 0$, an integrable function $g(y)$ will be called *α-fast decaying* on the positive half-axis if $\left|\int_0^{+\infty} e^{\alpha y_1}\, g(y_1)\, dy_1\right| < \infty$,; a function will be called α-fast decaying if it is fast decaying on both half-axes. For a function that is α-fast decaying on the positive half-axis

$$(\nabla_\alpha^{-2}\, g)(y) = \int_{+\infty}^{y} \frac{\sinh(\alpha(y-y_1))}{\alpha}\, g(y_1)\, dy_1 - E^+ e^{-\alpha\, y} \tag{C.2}$$

and for a function α-fast decaying on the negative half-axis the lower limit should be taken as $-\infty$ and the homogeneous solution part be taken in the form $E^- e^{\alpha\, y}$; for an α-fast decaying function both forms are admissible. In any of these cases, for general $g(y)$ only a decay of the type $\exp(-\alpha|y|)$ can be guaranteed (on the half-axis of decay) for the result $(\nabla_\alpha^{-2}\, g)(y)$.

It is important that the form (C.2) assumes a fixed constant multiple E^+ of the decaying homogeneous solution on the positive half-axis. The latter constant is free to be fixed when defining the inverse Laplacian, and is independent of $g(y)$. In contrast, the definition (C.1) which is valid simultaneously on both half-axes, can be put in the form (C.2) only if $g(y)$ is α-fast decaying , and E^+ and E^- are certain functionals of $g(y)$, namely

$$E^+[g] = \int_{-\infty}^{+\infty} \frac{e^{\alpha\, y}}{2\alpha}\, g(y)\, dy\,, \qquad E^-[g] = \int_{-\infty}^{+\infty} \frac{e^{-\alpha\, y}}{2\alpha}\, g(y)\, dy\,. \tag{C.3}$$

This follows from the requirement that the value of $\nabla_\alpha^{-2}\, g$ and its derivative should match at

the origin. It is convenient to rewrite it as

$$E^+ + E^- = \int_{-\infty}^{+\infty} \frac{\cosh(\alpha\, y)}{\alpha}\, g(y)\, dy\,, \qquad E^+ - E^- = \int_{-\infty}^{+\infty} \frac{\sinh(\alpha\, y)}{\alpha}\, g(y)\, dy\,. \tag{C.4}$$

The first form demonstrates the importance of the α-fast decaying requirement; the second shows that $E^+ = E^-$ for even $g(y)$, $E^+ = -E^-$ for odd $g(y)$.

b. Small-wavenumber expansion

Expanding the exponent in (C.1) in power series, it is straightforward to find a formal expansion of the integral operator (C.1). Its action on a given function $g(y)$ which is itself expanded in powers of α is then found to be

$$\begin{aligned} \nabla_\alpha^{-2}\,(\, g_0(y) \,+\, \alpha\, g_1(y) \,+\, \alpha^2 g_2(y) \,+\, \cdots\,) = -\frac{1}{2}\Big(\frac{1}{\alpha}\, I_0[\,g_0] \\ +\,(\,I_0[\,g_1] + I_1[\,g_0](y)) + \,\alpha\,(I_0[\,g_2] + I_1[\,g_1](y) + I_2[\,g_0](y)) \\ +\,\alpha^2\,(I_0[\,g_3] + I_1[\,g_2](y) + I_2[\,g_1](y) + I_3[\,g_0](y)) \,+\, \cdots\Big) \end{aligned} \tag{C.5}$$

with the functional I_0 and the operators I_n, $n = 1, 2, \ldots$, defined by formally comparing coefficients at equal powers of α. Their explicit form is

$$I_0[\,g(\cdot)\,] = \int_{-\infty}^{+\infty} g(y)\, dy\,, \qquad I_n[\,g(\cdot)\,](y) = \frac{(-)^n}{n!} \int_{-\infty}^{+\infty} g(y_1)\, |y - y_1|^n dy_1\,, \qquad n \geq 1\,. \tag{C.6}$$

The issue of convergence in (C.5) is beyond our present scope.

Appendix D Integrals of the type $I_k[\,h_n\,]$

In manipulations required for the small wavenumber asymptotic analysis, integrals of the type $I_k[\,h_n\,]$ with I_k defined by (C.6) in Appendix C which arise from the explicit expansion of the inverse Laplacian, have to be frequantly evaluated. Their explicit values are given below. In their derivation some properties of the Hermite functions considered in Appendix B are used. These concern the integrals of such functions (B.9) and the explicit relations between them which follow from (B.8), and are summarized for the present purposes by

$$\begin{aligned} h_1(y) &= -y\, h_0(y)\,, & h_2(y) &= (y^2 - 1) h_0(y)\,, \\ h_3(y) &= -(y^3 - 3y) h_0(y) & &= -(y^3 h_0(y) + 3h_1(y))\,, \\ h_4(y) &= (y^4 - 6y^2 + 3)\, h_0(y) & &= y^4 h_0(y) - 6h_2(y) - 3h_0(y)\,. \end{aligned} \tag{D.1}$$

Formula (C.5) suggests that it would be convenient to consider instead of I_k the operators

$$I_k^*[\,g(\cdot)\,] = \frac{(-)^k}{2} I_k[\,g(\cdot)\,] = \frac{1}{k!\,2} \int_{-\infty}^{+\infty} g(y_1)\, |y - y_1|^k dy_1\,. \tag{D.2}$$

The following operator appears in the derivations

$$I^\infty[\,g(\cdot)\,](y) = \frac{1}{2}\Big(\int_{-\infty}^{y} g(y_1)\, dy_1 + \int_{+\infty}^{y} g(y_1)\, dy_1\Big) \tag{D.3}$$

so that for functions $g(y)$ which have finite asymptotic values at infinity one has

$$I^{\infty}[\,g'(\cdot)\,](y) = g(y) \qquad \text{if} \qquad g(+\infty) + g(-\infty) = 0\,. \tag{D.4}$$

This is the case when $g = h_n$, $n = -1, 0, 1, 2, \ldots$. With these remarks, we apply $I_k^{\star}[\,h_n\,]$ for as many $n = 0, 1, \ldots$ as needed for the analysis, and for $k = 1, 2, 3$ successively.

First consider $k = 1$. Starting with $n = 0$, one observes upon expanding terms and substituting $-y_1\, h_0(y_1) = h_1(y_1)$, that

$$\begin{aligned} I_1^{\star}[\,h_0\,] &= \frac{1}{2}\left(\int_{-\infty}^{y} (y - y_1)\, h_0(y_1)\, dy_1 + \int_{+\infty}^{y} (y - y_1)\, h_0(y_1)\, dy_1\right) \\ &= I^{\infty}[\,(y - y_1) h_0(\cdot)\,](y) = y\, I^{\infty}[\,h_0(\cdot)\,](y) + I^{\infty}[\,h_1(\cdot)\,](y) \\ &= y\, h_{-1}(y) + h_0(y)\,, \end{aligned}$$

where (D.4) was applied at the last stage. Similarly, using (D.1) to substitute $-y_1\, h_1(y_1) = h_2(y_1) + h_0(y_1)$ one finds that $I_1^{\star}[\,h_1\,] = y\, h_0(y) + (h_1(y) + h_{-1}(y))$. To summarize,

$$\frac{1}{2}\int_{-\infty}^{+\infty} |y - y_1|\, h_0(y_1)\, dy_1 = y\, h_{-1}(y) + h_0(y)\,, \tag{D.5}$$

$$\frac{1}{2}\int_{-\infty}^{+\infty} |y - y_1|\, h_1(y_1)\, dy_1 = h_{-1}(y)\,. \tag{D.6}$$

The calculations of $I_2^{\star}[\,h_n\,]$ are simpler. To start with $n = 0$, one observes that

$$\begin{aligned} I_2^{\star}[\,h_0\,] &= \frac{1}{4}\left(y^2 \int_{-\infty}^{+\infty} h_0(y_1)\, dy_1 - 2y \int_{-\infty}^{+\infty} y_1\, h_0(y_1)\, dy_1 + \int_{-\infty}^{+\infty} y_1^2\, h_0(y_1)\, dy_1\right) \\ &= \frac{y^2 + 1}{4} \int_{-\infty}^{+\infty} h_0\, dy_1 = \frac{y^2 + 1}{2}\,, \end{aligned}$$

where (D.1) was used. Similarly,

$$\begin{aligned} I_2^{\star}[\,h_1\,] &= \frac{1}{4}\left(y^2 \int_{-\infty}^{+\infty} h_1(y_1)\, dy_1 - 2y \int_{-\infty}^{+\infty} y_1\, h_1(y_1)\, dy_1 + \int_{-\infty}^{+\infty} y_1^2\, h_1(y_1)\, dy_1\right) \\ &= \frac{1}{4}\left(2y \int_{-\infty}^{+\infty} (h_2 + h_0)\, dy_1 + \int_{-\infty}^{+\infty} (h_3 + 3\, h_1)\, dy_1\right) = y\,, \\ I_2^{\star}[\,h_2\,] &= \frac{1}{4}\left(y^2 \int_{-\infty}^{+\infty} h_2(y_1)\, dy_1 - 2y \int_{-\infty}^{+\infty} y_1\, h_2(y_1)\, dy_1 + \int_{-\infty}^{+\infty} y_1^2\, h_2(y_1)\, dy_1\right) \\ &= \frac{1}{2}\left(2y \int_{-\infty}^{+\infty} (h_3 + 4\, h_1)\, dy_1 + \int_{-\infty}^{+\infty} (h_4 + 5\, h_2 + 2\, h_0)\, dy_1\right) = 2\,. \end{aligned}$$

To summarize for $k = 2$,

$$\frac{1}{4}\int_{-\infty}^{+\infty} (y - y_1)^2\, h_0(y_1)\, dy_1 = \frac{y^2 + 1}{2}\,, \tag{D.7}$$

$$\frac{1}{4}\int_{-\infty}^{+\infty} (y - y_1)^2\, h_1(y_1)\, dy_1 = y\,, \tag{D.8}$$

$$\frac{1}{4}\int_{-\infty}^{+\infty} (y - y_1)^2\, h_2(y_1)\, dy_1 = 2\,. \tag{D.9}$$

Calculations for $k=3$ is similar to those for $k=1$. For $h_1(y)$, transforming $y^n h_1(y)$ according to (D.1), one finds

$$
\begin{aligned}
I_3^{\star}[\,h_1\,] &= \frac{1}{12}\left(\int_{-\infty}^{y}(y-y_1)^3\,h_1(y_1)\,dy_1 + \int_{+\infty}^{y}(y-y_1)^3\,h_1(y_1)\,dy_1\right), \\
&= \frac{1}{6}\Bigg(y^3\,I^{\infty}[\,h_1(\cdot)\,](y) \;-\; 3y^2 I^{\infty}[\,-(h_2+h_0)(\cdot)\,](y) \\
&\qquad + 3y\,I^{\infty}[\,(h_3+3\,h_1)(\cdot)\,](y) \;-\; I^{\infty}[\,-(h_4+6\,h_2+3\,h_0)(\cdot)\,](y)\Bigg), \\
&= \frac{1}{6}\Bigg(y^3 h_0(y) \;+\; 3y^2(h_{-1}(y)-y\,h_0(y)) \\
&\qquad + 3y\,(y^2+2)\,h_0(y) \;+\; (3\,h_{-1}(y) - (y^3+3y)\,h_0(y))\Bigg), \\
&= \frac{1}{2}\Big((y^2+1)\,h_{-1}(y) - h_1(y)\Big).
\end{aligned}
$$

Thus, one has that

$$
\frac{1}{6}\int_{-\infty}^{+\infty}|y-y_1|^3\,h_1(y_1)\,dy_1 = (y^2+1)\,h_{-1}(y) - h_1(y). \tag{D.10}
$$

Finally, the following relations, derived from (D.6),(D.8),(D.10) respectively by changing the order of integration, are used in the asymptotic analysis

$$
\frac{1}{2}\int_{-\infty}^{+\infty}dy\;h_1(y)\int_{-\infty}^{+\infty}dy_1\;|y-y_1|\;g(y_1) = \int_{-\infty}^{+\infty}h_{-1}(y)\;g(y)\;dy, \tag{D.11}
$$

$$
\frac{1}{4}\int_{-\infty}^{+\infty}dy\;h_1(y)\int_{-\infty}^{+\infty}dy_1\;(y-y_1)^2\,g(y_1) = \int_{-\infty}^{+\infty}y\;g(y)\;dy, \tag{D.12}
$$

$$
\frac{1}{6}\int_{-\infty}^{+\infty}dy\;h_1(y)\int_{-\infty}^{+\infty}dy_1\;|y-y_1|^3\,g(y_1) = \int_{-\infty}^{+\infty}\Big((y^2+1)\,h_{-1}(y)-h_1(y)\Big)\;g(y)\,dy. \tag{D.13}
$$

References

[1] Tanaka,M. and Kida,S. (1993), "Characterization of vortex tubes and sheets", *Phys.Fluids A*, 5, No.9, p.2079.

[2] Kida,S. and Tanaka,M. (1994), "Dynamics of vortical structures in a homegeneous shear flow", *J.Fluid Mech.*, 274, p.43.

[3] Rogers,M.M. and Moser,R.D. (1992), "The three-dimensionsl evolution of a plane mixing layer: the Kelvin-Helmholtz rollup", *J.Fluid Mech.*, 243, p.183.

[4] Vincent,A. and Meneguzzi,M. (1991), "The spatial structure and statistical properties in three-dimensional turbulence.", *J.Fluid Mech.*, 225, p.1.

[5] Metcalfe,R.,W., Orszag,S.A., Brachet,M.C., Menon,S., Riley,J.J. (1987), "Secondary instability of a temporally growing mixing layer", *J.Fluid Mech.*, 184, p.207.

[6] Corcos,G.M. and Lin,S.J. (1984), "The Mixing layer: deterministic models of a turbulent flow. Part 2. The origin of of the three-dimensional motion.", *J.Fluid Mech.*, 139, p.67.

[7] Lin,S.J. and Corcos,G.M. (1984), "The Mixing layer: deterministic models of a turbulent flow. Part 3. The effect of plane strain on the dynamics of streamwise vortices", *J.Fluid Mech.*, 141, p.139.

[8] Neu,J.C. (1984), "The dynamics of stretched vortices", *J.Fluid Mech.*, 143, p.253.

[9] Robinson,A.C. and Saffman,P.G. (1984), "Stability and Structure of Stretched Vortices", *Stud.Appl.Math.*, p.163.

[10] Tatsumi,T. and Gotoh,K. (1960), "The stability of free boundary layers between two uniform streams", *J.Fluid Mech.*, 7, p.433.

[11] Betchov,R. and Szewczuk,A. (1963), "Stability of a Shear Layer between Parallel Streams", *Phys.Fluids*, 6(10), p.1391.

[12] Drazin,P.G. and Reid,W.H. (1981), "Hydrodynamic Stability", Cambridge Univ.Press.

[13] Criminale,W.O., Jackson,T.L., Lasseigne,D.G. (1994), "Evolution of disturbances in stagnation-point flow", *J.Fluid Mech.*, 270, p.331.

[14] Wilson,S.D.R. and Gladwell,I. (1977), "The stability of a two-dimensional stagnation flow to three-dimensional disturbances", *J.Fluid Mech.*, 84, p.517.

[15] Passot,T., Politano,H., Sulem,P.L., Angilella,J.R., Meneguzzi,M. (1994), "Instability of strained vortex layers and vortex tube formation in homogeneous turbulence", *J.Fluid Mech.*, 282, p.313.

[16] Sherman,F.S. (1990), "Viscous Flow", McGraw-Hill Book Co.

[17] Batchelor,G.K. (1967), "An Introduction to Hydrodynamics", Cambridge Univ.Press.

[18] Howard,L.N. (1964), "The Number of Unstable Modes in Hydrodynamic Stability Problems", *Journal de Mécanique*, Vol.3, No.4, p.433.

[19] Lin,C.C. (1967), "The Theory of Hydrodynamic Stability", 2nd ed., Cambridge Univ.Press.

[20] Kerr,O. and Dold,J.W. (1994), "Periodic steady vortices in a stagnation-point flow", *J.Fluid Mech.*, 276, p.307.

[21] Abramovitz,M. and Stegun,I.A., ed. (1964), "Handbook of Mathematical Functions", Dover, New York, 1972.

α	0.0006	0.001	0.003	0.006	0.01	0.03	0.06
R	1.00101	1.00169	1.005095	1.01023	1.01713	1.05266	1.10941
α	0.1	0.2	0.3	0.4	0.5	0.6	0.7
R	1.19242	1.44796	1.80876	2.36935	3.40280	6.09349	25.796
R	1.1	1.2	1.3	1.5	2	3	4
α	0.05518	0.10344	0.14590	0.21693	0.33994	0.46924	0.53399
R	6	8	10	15	20	30	40
α	0.59803	0.63031	0.65002	0.67690	0.69063	0.70457	0.7116

Table 1: Typical wavenumber and Reynolds number couples on the neutral curve.

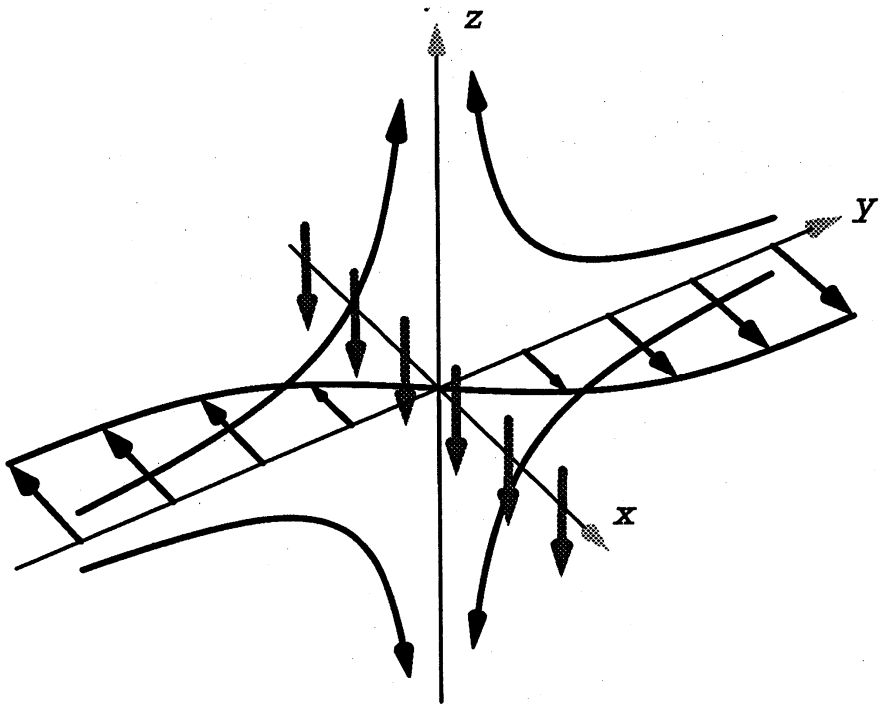

Figure 1: Geometry of the Burgers vortex layer. Gray arrows stand for vorticity, black straigt arrows for shear layer velocity. The direction of irrotational strain flow is indicated on its streamlines.

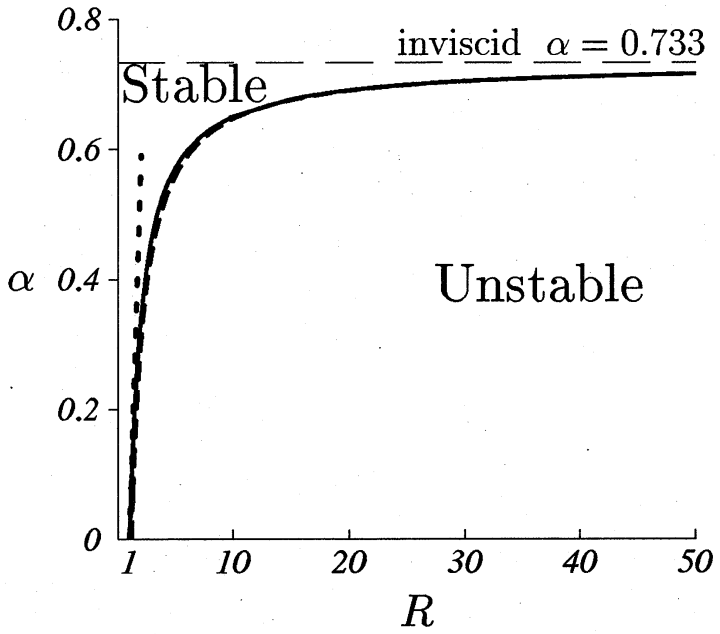

Figure 2: The neutral curve. A dashed curve shows the large-Reynolds-number asymptotics approximation and a dotted line the small-wavenumber approximation; a horizontal line marks the inviscid critical wavenumber

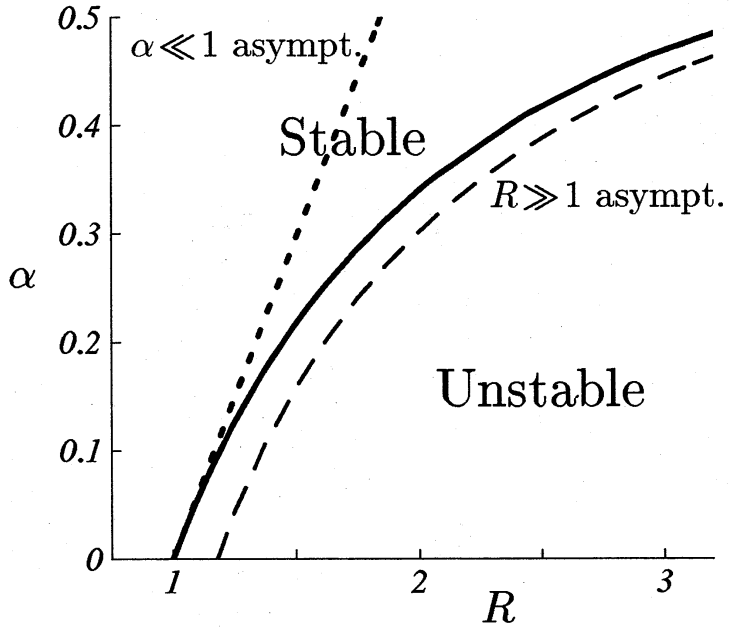

Figure 3: The neutral curve in the small-wavenumber end.

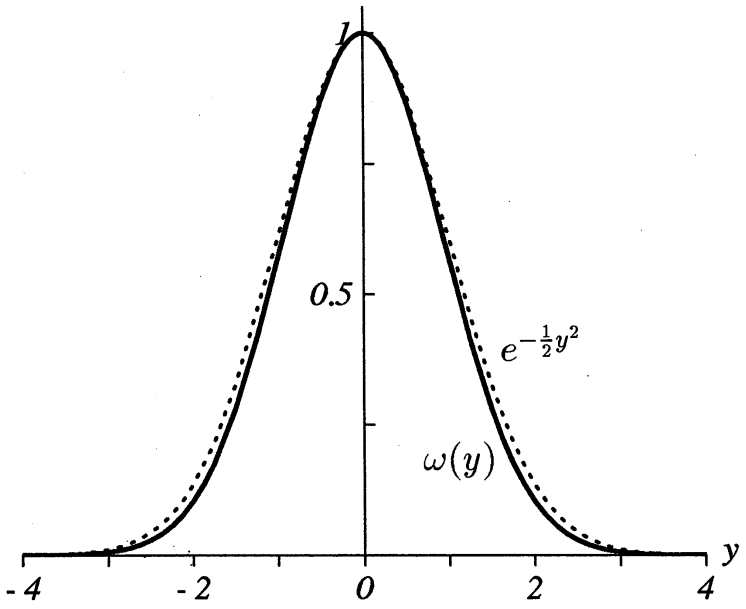

Figure 4: Neutral mode vorticity in the inviscid limit. A dotted line shows $e^{-\frac{1}{2}y^2}$.

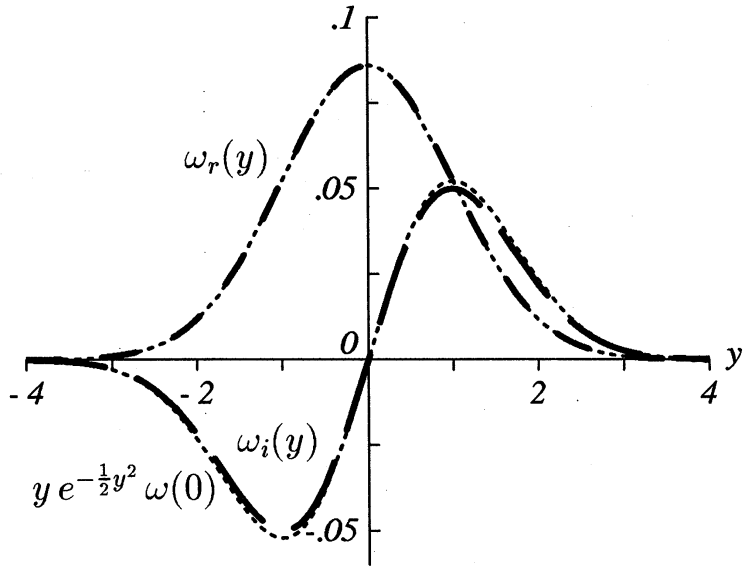

Figure 5: Neutral mode vorticity for $\alpha = 0.1$. The real part is plotted with shorter and the imaginary part with longer dashes. Dotted lines show $e^{-\frac{1}{2}y^2}\,\omega(0)$ and $y\,e^{-\frac{1}{2}y^2}\,\omega(0)$.